

GORAM: Graph-oriented ORAM for Efficient Ego-centric Queries on Federated Graphs

Xiaoyu Fan
fxy23@mails.tsinghua.edu.cn
IIS, Tsinghua University

Xiaowei Zhu
robert.zxw@antgroup.com
Ant Group

Kun Chen
ck413941@antgroup.com
Ant Group

Yunyi Chen
cyy23@mails.tsinghua.edu.cn
Tsinghua University

Wei Xu
weixu@tsinghua.edu.cn
IIS, Tsinghua University

Jiping Yu
yjp19@mails.tsinghua.edu.cn
Tsinghua University

Huanchen Zhang
huanchen@tsinghua.edu.cn
IIS, Tsinghua University

Abstract

Ego-centric queries, focusing on a target vertex and its direct neighbors, are essential for various applications. Enabling such queries on graphs owned by mutually distrustful data providers, without breaching privacy, holds promise for more comprehensive results.

In this paper, we propose GORAM, a graph-oriented data structure that enables efficient ego-centric queries on federated graphs with strong privacy guarantees. GORAM is built upon *secure multi-party computation (MPC)* and ensures that no single party can learn any sensitive information about the graph data or the querying keys during the process. However, achieving practical performance with privacy guaranteed presents a challenge. To overcome this, GORAM is designed to partition the federated graph and construct an *Oblivious RAM (ORAM)*-inspired index atop these partitions. This design enables each ego-centric query to process only a single partition, which can be accessed fast and securely.

To evaluate the performance of GORAM, we developed a prototype querying engine on a real-world MPC framework. We conduct a comprehensive evaluation with five commonly used queries on both synthetic and real-world graphs. Our evaluation shows that all benchmark queries can be completed in just 58.1 milliseconds to 35.7 seconds, even on graphs with up to 41.6 million vertices and 1.4 billion edges. To the best of our knowledge, this represents the first instance of processing billion-scale graphs with practical performance on MPC.

1 Introduction

Graphs, with their inherent interconnections, have played an important role in various areas, including financial industry, social networks, public health, *etc.* One of the crucial applications on graphs is *ego-centric* queries, which focus on a target vertex and all its directly connected neighbors. For example, by analyzing the relations among suspicious accounts, commercial banks can achieve efficient detection of money laundering from the transaction graphs [45, 53]. Social network giants use graphs to model and manage users and their relationships. As LinkBench [39] reports, ego-centric reads for accounts, relations, and neighbor-statistics on the given account constitute 12.9% and 55.6% of the total processed queries from Meta. In addition, quick identification of people who

have been exposed to an infected person through the contact graph has played an important role during the COVID-19 pandemic [42].

When the underlying graph is distributed across multiple data providers—a common occurrence in the real world—conducting ego-centric queries on the federated graphs is promising for more comprehensive and valuable results. However, this poses significant privacy challenges. As demonstrated in the above motivating examples, both the graph data and the querying targets contain sensitive information. Therefore, it is crucial to keep both of them private with strong guarantees. One mainstream way to implement private queries on federated data is to use *secure multi-party computation (MPC)* [66] throughout the query process [11, 12, 16, 40, 59]. MPC is a cryptographic technique that allows multiple parties to jointly compute a function on their private inputs, while keeping the inputs secret without a trusted third party. Similar to the state-of-the-art secure tabular data analytics framework [40], we encode the graph data and the querying keys as *secret shares*, ensuring that no single party can learn any sensitive information about the query keys or the graph data, including the existing vertices and edges, the number of the neighbors *etc.*

After providing theoretically sound privacy guarantees, the next challenge is to achieve practical performance on real-world graphs. Based on the prior secure graph processing literatures using MPC [10, 15, 51], it is straightforward to apply the existing secure graph data structures, *i.e.*, *secure adjacency matrix* [15] or *secure list* [10, 46, 47, 51], to implement ego-centric queries. However, these data structures either impose impractical space overheads or require scanning the entire graph for each query, making them applicable only to small-scale graphs. Blanton *et al.* [15] propose to store the graph in a secret-shared adjacency matrix, which requires at least $O(|V|^2)$ space complexity, where $|V|$ is the number of vertices. The quadratic space overhead is impractical for real-world graphs. For example, Twitter [17], which contains more than 41.6 million vertices, would require more than 1.6 *petabytes* of storage assuming each matrix cell only requires 1 byte. Nayak *et al.* [51], on the other hand, propose to store the graph in a secret-shared list, which reduces the space overhead to $O(|V| + |E|)$, where $|E|$ is the number of edges. This representation is space-efficient because $|V| + |E|$ is usually much smaller than $|V|^2$ for real-world graphs [22].

However, this data structure necessitates entire graph scanning for each query, leading to prohibitive costs for large graphs.

Despite the above flaws, we found that the above data structures hold potential to implement practical ego-centric queries. By leveraging *Oblivious RAM (ORAM)* [27, 67], a secure indexing mechanism in MPC that allows accessing the i th element of an array without revealing the index i in sub-linear complexity, it is possible to locate all the neighbors of a target vertex v from the adjacency matrix to achieve sub-linear query processing complexity, *i.e.*, accessing the $v * |V|, v * |V| + 1, \dots, (v + 1) * |V| - 1$ elements of the adjacency matrix to obtain the v -th row while keeping the target v secret. The secure list, on the other hand, provides promising scalability to real-world graphs because of its efficient space utilization. The above two data structures essentially store the graph in two extreme ways, one is (possibly) query-efficient but space-inefficient, and the other is space-efficient but query-inefficient. Inspired by the above contrast, we propose GORAM, a graph-oriented data structure that combines the advantages of the adjacency matrix and the list to support efficient ego-centric queries on large-scale federated graphs with strong privacy guarantees.

To achieve sub-linear query processing complexity, GORAM segments the vertices into multiple chunks, and then splits the graph into a “matrix” of edge lists. Each edge list contains all the edges starting from source vertices in the row’s chunk and destinations in the column’s. Intuitively, this organization leverages the property of adjacency matrix that allows accessing all the neighbors of a vertex in sub-linear time, and utilizes the space efficiently by storing each matrix cell as an edge list. In this way, we split the graph into multiple *partitions*, satisfying that all the information needed for each ego-centric query is contained in *exactly* one partition. With additional padding, we can theoretically guarantee that no single party can tell the difference between the partitions. This design enables GORAM to reduce the to-be-processed graph size for each query, while guaranteeing strong privacy (Section 4.1). To enable efficient and secure access to the target partition, GORAM employs an indexing layer on top of the partitions, inspired by ORAM [67]. The indexing layer maintains a secret mapping from the vertex ID or edge IDs to the location of the corresponding partition. Just like the ORAM accessing the i th element in an array, GORAM can access the target partition efficiently without disclosing any information about the querying keys, *i.e.*, specific IDs (Section 4.5). Besides, GORAM incorporates several optimizations to accelerate the initialization and partition accesses stages, including parallelisms (Section 4.6) and a constant-round shuffling protocol (Section 5).

Based on GORAM, we can easily implement crucial queries easily. We build a prototype querying engine on top of the ABY3 [49] MPC framework and implement five ego-centric queries, including *edge existence, 1-hop neighbors, neighbors statistics etc.*, covering all the queries¹ listed in LinkBench [39] (Section 6). Then, we evaluate the above queries on five synthetic graphs with varied distributions and three real-world graphs. Results in Section 7 show remarkable efficiency and scalability of GORAM. On synthetic graphs with up to 2^{15} vertices, all the basic queries are finished within 132.8 milliseconds, outperforming queries based on prior secure graph

data structures by *2 to 3 orders of magnitude*. For a real-world graph, Twitter [17], with more than 41.6 *million* vertices and 1.4 *billion* edges, the results can be obtained within 35.7 seconds, and the fastest edge existence query only takes 58.1 milliseconds. Also, the initialization of GORAM only requires 3.0 minutes. To the best of our knowledge, GORAM is the first step towards querying graphs scaling to more than one *billion* edges in secure computations - a scale 2 orders of magnitude larger than the prior arts [10, 47].

In summary, our contributions include:

- 1) We propose GORAM, a graph-oriented data structure to support efficient sub-linear ego-centric queries on federated graphs guaranteeing strong privacy.
- 2) We design comprehensive optimizations to enable practical performance on large-scale graphs, including local processing, lifecycle parallelisms and a constant-round shuffling protocol.
- 3) A prototype querying engine based on GORAM is developed on real-world MPC framework and evaluated comprehensively using five commonly-used queries on eight synthetic and real-world graphs, demonstrating remarkable effectiveness, efficiency, and scalability.

2 Background

2.1 Secure Multi-party Computation (MPC)

Secure Multi-party Computation (MPC) is a cryptographic technique that allows multiple distrusting parties to jointly compute a function on their private inputs, ensuring that all the information remains secret except for the result.

Secret sharing is one of the most fundamental techniques in MPC [66]. A (t, n) -*secret sharing* schema splits any sensitive data x to n parties, satisfying that any t parties can reconstruct x while fewer than t parties learn nothing about x . GORAM adopts the $(2, 3)$ -secret sharing for efficiency, similar to prior works [10, 25, 40, 49]. Specifically, x is split into (x_1, x_2, x_3) , satisfying that each $x_i, i \in \{1, 2, 3\}$ is uniformly random and $x \equiv x_1 \oplus x_2 \oplus x_3$. \oplus denotes the bitwise XOR. Each party owns two shares (x_i, x_{i+1}) where the indices are wrapped around 3. Therefore, any party learns nothing about x while any two parties can perfectly reconstruct x . This format is *boolean* secret share, and it is the primary format used in GORAM. We denote the boolean secret shares of x as $\llbracket x \rrbracket$. GORAM also transforms $\llbracket x \rrbracket$ into *arithmetic* shares sometimes for efficiency, *i.e.*, $x \equiv x_1 + x_2 + x_3 \pmod{2^k}$, denoted as $\llbracket x \rrbracket^A$.

Secure operations. With the secret shares $\llbracket x \rrbracket$ and $\llbracket y \rrbracket$, the parties can collaboratively compute the shares of the result $\llbracket z \rrbracket$ for a variety of commonly-used operations (op) using MPC protocols (OP). The protocols guarantee that for $z = \text{op}(x, y)$, $\llbracket z \rrbracket = \text{OP}(\llbracket x \rrbracket, \llbracket y \rrbracket)$ (correctness), and the parties learn nothing about the secret inputs during the protocol execution (privacy). Numerous well-developed MPC protocols exist for basic operations, including bitwise XOR, AND, OR, addition(+), multiplication(\times), comparisons($>$, \geq , $=$) and transformations between $\llbracket x \rrbracket$ and $\llbracket x \rrbracket^A$ [23, 49]. Except for XOR on boolean shares and addition on arithmetic shares, all other operations require at least one round of communication among the computing parties. Consequently, batching multiple operations into a single vector can effectively offset the communication latency, thus improving performance [34, 40, 49]. By composing these basic

¹Specifically, query in this paper refers to static query, and we do not support real-time updates yet.

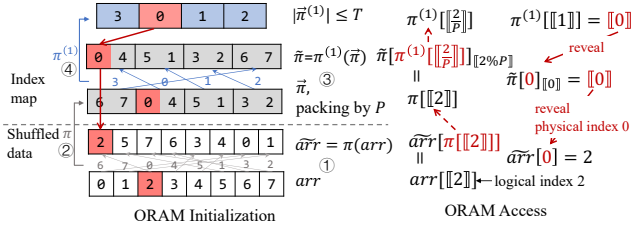


Figure 1: Square-root ORAM Workflow ($P = 2, T = 4$)

operations, we can design high-level secure algorithms like machine learning [28, 35, 54] and relational queries [12, 40, 59]. GORAM adopts all its secure protocols from the efficient ABY3 [49] MPC framework, and takes the advantage of batching during query processing. Note that GORAM is agnostic to the underlying protocols, and can be easily extended to use other MPC protocols.

Security guarantees. MPC guarantees the privacy of the inputs and the correctness of the outputs against a specific *adversary model*. The adversary model describes how the adversary can corrupt the joint parties. Common classifications include *semi-honest vs. malicious*, determined by whether the corrupted parties can deviate from the given protocols; and *honest- vs. dishonest- majority*, contingent on the corruption proportion. The underlying MPC protocol of GORAM is secure against a semi-honest and honest-majority adversary, keeping align with the prior works [10, 25, 40, 49]. As there are only three parties, honest-majority is equivalent to *non-colluding*, i.e., only one party can be corrupted.

2.2 Oblivious RAM (ORAM)

Oblivious RAM (ORAM), introduced by Goldreich and Ostrovsky [27], implements oblivious *indexing*, i.e., accessing the i th element in an array without scanning the entire array while keeping i secret. ORAM brings two promising properties in building efficient graph query engines. Firstly, it ensures that the access patterns are hidden, i.e., for *any* two indices i, j , servers performing the access can not distinguish whether the index is i or j , protecting the privacy of the query keys. Secondly, it enables sub-linear-complexity accesses. This is essential for large-scale graphs because we can avoid a full graph scan for each query.

The original ORAM, e.g., Path ORAM [57], is designed for the *client-server* scenario, where a single client stores and retrieves her own private data on an untrusted server [27]. However, it is not suitable for our case because the underlying data is contributed by multiple data providers instead of a single one. Also, the party who wishes to access the data may not be the data provider.

Distributed ORAM (DORAM) is proposed to support the case where a group of computation servers together hold an array of secret-shared data. The servers can jointly access the target secret element given the secret-shared index [44], i.e., compute $[[arr[i]]] = [[arr]][[i]]$. DORAM does not require the data is owned and accessed by a single data provider, thereby enabling the cases where data is contributed by multiple data providers. DORAM is currently an active research area and there are several efficient implementations [18, 24, 25, 58, 67]. The indexing layer of GORAM is inspired by DORAM and it is agnostic to the specific DORAM implementations. For sub-linear access complexity and strong privacy guarantee,

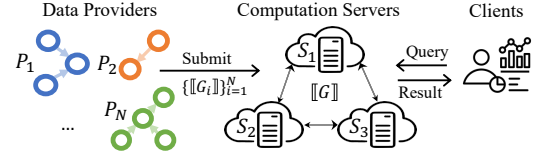


Figure 2: Logical Roles

GORAM adopts the classic Square-root ORAM [67] as the DORAM protocol in the indexing layer. The other DORAM implementations are discussed in Section 8.

Square-root ORAM. The workflow of Square-root ORAM [67] is illustrated in Figure 1. The key idea is to shuffle the original data (arr) according to a random permutation π , then build an index map on π that translates the secret logical index $[[i]]$ to the plaintext physical index p in the shuffled data, satisfying that $arr[p] \equiv \overline{arr}[i]$. Specifically, after shuffling $\overline{arr} = \pi(arr)$ (step ①), ORAM stores the permutation representation $\tilde{\pi} = \{\pi^{-1}(0), \pi^{-1}(1), \dots, \pi^{-1}(n-1)\}$ in secret shares (step ②). Each $\tilde{\pi}_i$ records the location of $arr[i]$ in \overline{arr} after applying π . The index map of π is constructed as a recursive ORAM, where P successive elements of $\tilde{\pi}$ are packed together as a single element and then build an ORAM for the $\frac{|\tilde{\pi}|}{P}$ elements recursively (step ③ to ④), until the ORAM size is reduced to no greater than T elements. The access process is also recursive, as demonstrated in Figure 1. For example, to access the 2nd element in arr (i.e., $arr[2]$), it is equivalent to accessing the $(\pi[2])$ th element in the shuffled $\overline{arr}[\pi[2]]$. For $\pi[2]$, we then access the $\tilde{\pi}[\pi^{(1)}[\frac{2}{P}]]_{2\%P}$ in $\tilde{\pi}$ recursively until the last layer.

Intuitively, each different logical index $[[i]]$ reveals a different random index, thereby keeping the access pattern private. However, identical logical indices lead to the same random indices, which breaches privacy. To address this issue, Square-root ORAM employs a *stash* in each layer that stores the accessed element each time. For each logical index, we first scan the stash to obtain a potential match, if it is not found, we access the ORAM using the given logical index, otherwise we access the ORAM using an unused index to hide the access pattern. The stash grows with each access and we need to rebuild the whole ORAM once the stash is full. The average access complexity of successive T elements is $O(PT \log(\frac{n}{T}))$, where n is the total number of elements in the ORAM. By default, $T = \sqrt{n}$. In the remainder of this paper, any references to ORAM indicate Square-root ORAM unless stated otherwise.

3 Overview

A system that supports real-world *private ego-centric* queries on federated graphs must satisfy the following three requirements:

1) *Functionality*: considering the diverse real-world applications, we should support *any* number of data providers, and handle *arbitrary* ego-centric queries, i.e., any queries on the sub-graph encompassing the target edge or vertex and all its direct neighbors.

2) *Privacy*: during the querying process, we should keep two information private: a) the querying keys of the clients, i.e., the target vertices or edges; and b) the private graph of the data providers. Specifically, no *crucial* information about the private graph, including the existence of specific vertices and edges, should be leaked. An additional requirement for the parties obtaining the query result

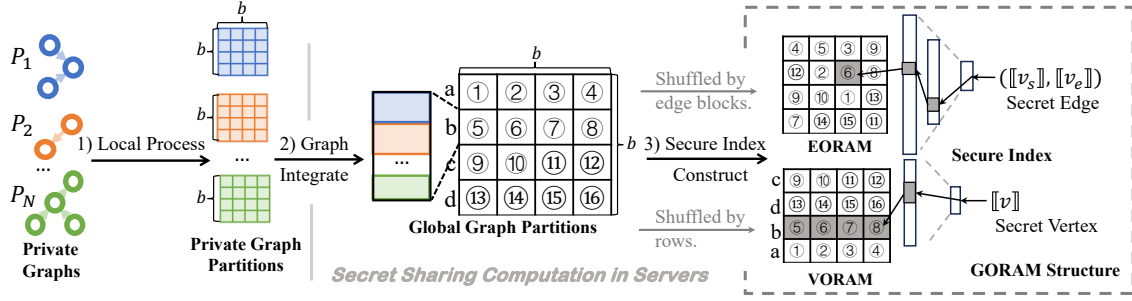


Figure 3: GORAM Initialization and Structure Overview

is that they cannot tell which provider contributes to the result. Section 3.4 shows the privacy guarantees GORAM provides.

3) *Efficiency and scalability*: A practical system should be capable of generating real-time responses for each query, even on graphs with edges scaling up to billions. In practical terms, we anticipate responses within a few seconds on graphs with billion-scale edges, thereby necessitating sub-linear complexity.

3.1 Formalization

Roles. There are three types of roles in the querying process, as shown in Figure 2: arbitrary number of *data providers*, who own private graphs; three *computation servers*, who carry out the secure query processing, during which they communicate with each other through secure channels *e.g.*, TLS; and an arbitrary number of *clients* who submit queries to the computation servers and receive the results. Similar to [40], the roles are decoupled. Each party can hold any combination of *different* roles, *e.g.*, one party can be both a data provider and a computation server. By limiting the secure computation on three computation servers, we avoid the need for coordination among the joint data providers, enabling scalability to *any* number of data providers.

Private ego-centric queries on federated graphs. We assume a *global* directed graph $G = (V, E)$ is distributed among N data providers $P_i, i \in [N], [N] = \{1, 2, \dots, N\}$. V and E denote the vertex and edge sets, respectively. Each edge $e \in E$ has a source and destination vertex, v_s and v_d . We assume the edges are different even if they have the same (v_s, v_d) , because they may contain different attributes in the real worlds (*e.g.*, timestamps [39]). For undirected graphs, we transform them into directed ones by representing each edge with two directed edges.

Each data provider P_i therefore owns a private graph $G_i = (V_i, E_i)$, satisfying that $V_i \subseteq V, E_i \subseteq E$ and $E = \cup_{i \in [N]} E_i$. The global vertex set V is public, enabling the clients to issue queries about the vertices they are interested in. Note that the vertices union $\cup_{i \in [N]} V_i \subseteq V$ is unnecessary for any role, and V can be the encoding space of the vertices. G_i should remain private during the process and therefore the global edge set E is private.

We assume three *semi-honest* computation servers $S_i, i \in [3]$, exist, holding the secret global graph $\llbracket G \rrbracket = (V, \llbracket E^+ \rrbracket)$, where $E^+ \supseteq E$ is a super-set of E because it may contain dummy edges for privacy. Each client can submit queries on the interested vertex $\llbracket v \rrbracket$ or edge $(\llbracket v_s \rrbracket, \llbracket v_d \rrbracket)$ to the servers and obtain the results, where v, v_s and $v_d \in V$, and the servers should return the result in a

timely manner with privacy requirements satisfied. Specifically, the client can conduct arbitrary ego-centric queries on a sub-graph $G_{\text{sub}} = \{V_{\text{sub}}, E_{\text{sub}}\}$ containing all the direct neighbors of the target vertex v and the corresponding edges (v, v^*) if $(v, v^*) \in E$, or all edges $(v_s, v_d) \in E$. For simplicity, we refer to both vertex- and edge-centric queries as ego-centric queries in the following.

3.2 Strawman Solutions

In the literature of secure graph processing, two classic data structures are used to present the secure graph, *i.e.*, *adjacency matrix* (*Mat*) [15] and *edge list* (*List*) [10, 46, 47, 51]. By adopting these two data structures, we can construct the secret-shared global graph $\llbracket G \rrbracket$ from the private graphs of the data providers and implement ego-centric queries through the following methods.

Based on Mat. With the public vertex set V , data providers can locally construct the $|V|^2$ adjacency matrix, encrypt it into the secret-shared matrix, and transfer the shares to the computation servers. The servers add up the secret matrices element-wise to form the secret matrix of the global graph G . Because *Mat* models the graph as a $|V| \times |V|$ matrix, we can adopt the ORAM atop of it to support efficient ego-centric queries. Specifically, we build two ORAMs, one is an ORAM over an array of $|V|$ matrix rows (adj-VORAM) and the other is over an array of $|V|^2$ matrix elements (adj-EORAM). For ego-centric queries about vertex v , we can access the $\llbracket i \rrbracket$ th row from the adj-VORAM. This row contains $|V|$ elements, each representing the edge number between v and $v_j, j \in [|V|]$; and for queries about edge (v_i, v_j) , we can access the element $\llbracket i * |V| + j \rrbracket$ from the adj-EORAM, which contains the number of edge (v_i, v_j) . Through ORAM, we can achieve $O(|V|)$ or $O(PT \log(\frac{|V|}{T}))$ complexity for each vertex- or edge-centric query, respectively. However, the major drawback is the $O(|V|^2)$ space cost, making it impractical for sparse graphs, which is unfortunately common in real-world applications [6, 22, 39, 65]. Also, we can not support arbitrary ego-centric queries, *e.g.*, statistic analysis, because we can not support the cases that the edges with the same start and end vertices contain different attributes. To support the cases directly, data providers can place multiple edges (v_i, v_j) with different attributes into the (i, j) th matrix cell. However, this would compromise privacy as the servers could infer which edge is more prevalent in the private graphs. To protect this information, we must pad each cell to align with the maximum one using dummy edges, which exacerbates the already considerable space cost.

Based on *List*. Each data provider P_i can encrypt their edges $(u, v) \in E_i$ into a secret-shared list, where each edge is represented as a tuple $(\llbracket u \rrbracket, \llbracket v \rrbracket)$, potentially with an additional field for attributes. The providers then send the secret lists to the computation servers, who merge the N secret lists to create the edge list of the global graph G . In this way, the only information leaked to the servers is the edge numbers. To protect the exact numbers, providers can append extra ϵ_i dummy edges, *i.e.*, $(\llbracket 0 \rrbracket, \llbracket 0 \rrbracket)$, before sending to the servers. Because all the edges are encrypted, and we have no knowledge about the existing vertices and edges, we can only scan the whole *List* for each ego-centric query, which introduces $O(|E|)$ complexity.

In summary, the above two methods contain theoretical limitations to satisfy the practical requirements. *List* requires scanning the whole edge list even if the query targets a single vertex/edge only, limiting the performance; *Mat* introduces impractical space cost and can not support arbitrary ego-centric queries.

3.3 GORAM Overview

Motivation and key idea. The above two data structures actually represent the graph in two extreme ways: *List* is space-efficient but slow for queries, while *Mat* is query-efficient but introduces impractical space cost. This contrast motivates us to design a data structure that strikes a balance between the two extremes and leverages the advantages of both. The high-level idea is to segment the vertices into multiple chunks and construct the graph into a “matrix” of edge lists. Intuitively, the matrix structure enables the establishment of ORAMs on top of the graph, circumventing the need for a full scan for each query. Simultaneously, the use of internal edge lists averts the $O(|V|^2)$ space complexity associated with the *Mat* structure. This balanced approach seeks to create a data structure that is both space- and query-efficient.

GORAM Overview. As shown in Figure 3, GORAM is a secret-shared data structure of the global graph $\llbracket G \rrbracket$, held by the computation servers. GORAM splits the public vertex set V into a set of b vertex chunks at first, and then splits the graph $\llbracket G \rrbracket$ into a “matrix” of b^2 blocks, each block contains *all* the edges starting from and ending in two specific vertex chunks; and each row of the blocks correspondingly contains *all* the direct neighbors of a specific vertex chunk. The block and row of blocks constitute the *partitions* for edge- and vertex-centric queries, respectively. GORAM then constructs $\llbracket G \rrbracket$ into VORAM and EORAM, which can securely access the partition given the secret vertex or edge. The indexing is achieved by modeling the partitions as ORAM, and we extend its functionality from accessing *array-of-elements* to *array-of-partitions*.

GORAM can be securely and efficiently initialized through three steps: 1) the data providers locally process their private graph into secret-shared partitions; 2) the computation servers integrate all the partitions of private graphs into the global graph $\llbracket G \rrbracket$; and 3) the computation servers construct the secure indices for the partitions. The details of GORAM are illustrated in Section 4.

Through GORAM, we can implement arbitrary and efficient ego-centric queries easily. For each query, the computation servers receive the secret edge or vertex from the client, access the corresponding partition through GORAM, process the partition for the

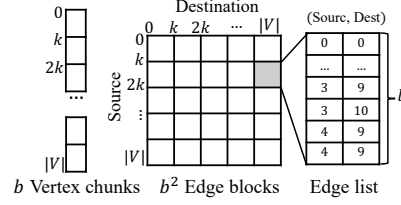


Figure 4: Graph Partition Structure ($k = 2$, $|V| = 10$)

given query, and return the result to the client. We provide five query examples in Section 6.

3.4 Privacy Guarantees

Threat model. Similar to the prior private data analytic applications [10, 11, 25, 40], GORAM focuses on withstanding a *semi-honest* and *non-colluding* adversary, who can compromise one computing party and see all of its internal states.

Privacy guarantees. GORAM provides two guarantees: 1) *query key privacy* of the client: no other party can learn anything about the client’s query key except the query type, *i.e.*, any other parties can only tell the query is about vertex or edge but nothing else; and 2) *graph privacy* of each data provider: no other party can learn any crucial information about the data provider’s private graph, *e.g.*, which vertices or edges are in the private graph, which vertices have higher degrees, or the attributes of each edge. Specifically, all other parties learn nothing about the private graph except the partition size, and this size can also be padded by the data providers. Additionally, the client who receives the query result learns nothing except the result, including which provider contributes to it.

4 Graph-Oriented ORAM (GORAM)

In this section, we introduce GORAM, including graph partitions (Section 4.1), GORAM initialization (Section 4.2 to Section 4.4), how to access partition securely through GORAM (Section 4.5), and parallelization (Section 4.6).

4.1 Graph Partitions

To satisfy the requirements in Section 3, GORAM organizes the graph into a $2d$ -partitioned data structure, as Figure 4 shows, which splits the graph into multiple blocks. This data structure groups successive k vertices into one chunk, forming $b = \lceil \frac{|V|}{k} \rceil$ chunks, according to the randomly shuffled IDs from the range $[|V|] = \{1, 2, \dots, |V|\}$. Then, it creates b^2 edge blocks for each pair of the chunks. Each edge block (i, j) contains all the edges $\{(v_s, v_d)\}$, where the source vertex v_s belongs to the i th chunk and the destination vertex v_d belongs to the j th chunk. Since the global vertex set is public, each data provider P_i can locally split the private graph G_i into the standard b^2 blocks given a configuration parameter k (Section 4.3). It is worth noting that each edge (v_s, v_d) , if it exists, is contained in a single edge block $(\lceil \frac{v_s}{k} \rceil, \lceil \frac{v_d}{k} \rceil)$; and for each vertex v , all the direct neighbors, specifically, outgoing neighbors in the case of directed graphs² are included in the $\lceil \frac{v}{k} \rceil$ th row (b blocks). Therefore, GORAM can answer each ego-centric query by

²If the bi-directional neighbors are interested, the in-going neighbors are included in the $\lceil \frac{v}{k} \rceil$ th column of the $2d$ partitioned graph.

Algorithm 1: Local Process

Global config: Vertex set V , configuration parameter k .
Inputs : Private graph $G_i = (V_i, E_i)$, $V_i \subseteq V$, for each data provider P_i .
Output : 2d-partitioned graph G_i .Block.

- 1 Computes the vertex chunk number $b = \lceil \frac{|V|}{k} \rceil$;
- 2 Initiates edge block G_i .Block as $b \times b$ empty vectors;
// Assign edges to the target blocks.
- 3 **for each edge** $(v_s, v_d) \in E_i$ **do**
- 4 Computes the start and end chunk IDs $s = \lceil \frac{v_s}{k} \rceil$ and $e = \lceil \frac{v_d}{k} \rceil$;
- 5 G_i .Block[s][e].append(v_s, v_d) *// Attributes can be included;*
- 6 **end**
// Sort and align each block.
- 7 Max block size $l_i \leftarrow \max(\{len(\text{block}), \forall \text{block} \in G_i$.Block\});
- 8 **for each edge block** $\in G_i$.Block **do**
- 9 Sort(block) using key $v_s || v_d$;
- 10 Pads $(l_i - len(\text{block}))$ empty edges $(0, 0)$ in the beginning to align with l_i ;
- 11 **end**
- 12 **return** G_i .Block;

processing the relevant blocks. The block and row of blocks are the graph *partition* for edge- and vertex-centric queries, respectively.

4.2 Local Process

Given a global configuration k , each data provider can independently construct the 2d-partitioned structure of their private graph G_i following Algorithm 1. The method of determining k is left in Section 4.3. Each P_i at first initializes b^2 edge blocks, denoted as G_i .Block, using the global V regardless of the vertices actually owned in the private vertex set V_i , where $b = \lceil \frac{|V|}{k} \rceil$. P_i then traverses the edge list E_i , pushing the edge into the corresponding edge block (s, d) if the edge (v_s, v_d) satisfies that $\lceil \frac{v_s}{k} \rceil = s$ and $\lceil \frac{v_d}{k} \rceil = d$. Afterward, each edge block is sorted using the key $v_s || v_d$ (i.e., concatenation of the source and destination vertices). A sorted order of each block is beneficial for some queries, e.g., the 1-hop neighbors, as discussed in Section 6. To protect the graph structure, each edge block should be aligned before being sent to the computation servers. Otherwise, even if the edges are encrypted, the computation servers can tell which group of vertices has stronger or weaker connections from the block sizes. Therefore, each data provider pads dummy edges, i.e., $(0, 0)$, to align all blocks to the maximum block size l_i . Note that l_i is the *only* information exposed about G_i , and each provider can pad it with extra dummy edges.

4.3 Global Integration

After the local process, each data provider P_i now transforms the private graph G_i into a $(b \times b \times l_i)$ 2d-partitioned G_i .Block. P_i then locally encrypts all the elements in G_i .Block into boolean secret shares, including all IDs and attributes, and transfers the shares to the corresponding computation servers.

After receiving the secret shares of N private graphs, i.e., $\llbracket G_i$.Block \rrbracket , $i \in [N]$, the computation servers integrate them to construct the secret partitioned global graph, $\llbracket G$.Block \rrbracket . Because each G_i .Block contains $b \times b$ sorted edge blocks, the computation servers

construct $\llbracket G$.Block \rrbracket by concatenating all the N secret graphs $\llbracket G_i$.Block \rrbracket , $i \in [N]$ through a $b \times b$ parallel *odd_even_merge_sort* network [36], i.e., merge sort each edge block in parallel. Finally, the computation servers construct the global 2d-partitioned secret graph $\llbracket G \rrbracket$, which contains a $(b \times b \times l)$ -sized $\llbracket G$.Block \rrbracket , $l = \sum_{i=1}^N l_i$ and each edge block is sorted.

Global configurations. As the prior processes show, it is necessary to pre-define a global configuration parameter k , i.e., the number of vertices to group in one chunk. This allows each data provider to organize the private graph into the 2d-partitioned format locally, and enables the computation servers to efficiently integrate these graphs. GORAM decides k intuitively by trying to let each row of the 2d-partition contain the smallest number of elements exceeding a threshold size B . This approach facilitates efficient *vectorized* processing of each partition, i.e., processing a batch of elements in a single vector operation, thereby effectively amortizing the communication latency of secure operations [34, 40, 49]. To efficiently compute k and protect the edge distribution information of each provider at the same time, GORAM determines k by assuming the edges are uniformly distributed among the public vertex set V . Therefore, each row of the 2d-partition is assumed to contain the same number of edges, i.e., $bl = \frac{|E|}{b} \approx \frac{k * |E|}{|V|}$. Then, GORAM computes k by solving the following optimization problem:

$$\min_k \frac{k * |E|}{|V|}, \quad s.t., \quad \frac{k * |E|}{|V|} \geq B, \quad (1)$$

and we obtain that the optimal $k = \frac{B * |V|}{|E|}$. Therefore, GORAM let the computation servers compute $\llbracket k \rrbracket = \frac{B * |V|}{\sum_{i=1}^N \llbracket |E_i| \rrbracket}$ in ciphertext to protect the exact edge numbers of each data provider, and send the secret shares of $\llbracket k \rrbracket$ to data providers, who can locally reveal k and construct the 2d-partitions.

4.4 Secure Index Construction

To enable efficient and secure access to the target partition for each query, GORAM employs a secure index layer on top of the partitions, inspired by ORAM.

Key idea of GORAM index. As we introduced in Section 2.2, the key idea of ORAM is to shuffle the original data (Arr) according to a random permutation π , and then build an index map of π that can translate the secret logical index $\llbracket i \rrbracket$ to the plaintext physical index p in the shuffled data ($ShufArr$). Intuitively, the shuffling process effectively uncorrelates the logical and physical indices, thus enabling direct access to the target element. The key idea of GORAM index is to replace the underlying *array of elements* with an *array of partitions*. This substitution becomes feasible once the partitions can be addressed by their locations in the array. Because the 2d-partitioned graph is already organized as an array of partitions and the location of each partition can be directly computed from the vertex ID or edge IDs, we can build the index map translating the logical index into the physical index of the partition.

GORAM index. We then model the partitioned graph $\llbracket G$.Block \rrbracket with two sub-ORAMs for vertex- and edge-centric queries, respectively: 1) VORAM models the 2d-partitioned graph as an array (Arr) of b partitions, each containing bl secret edges, i.e., one row of blocks in 2d-partition; and 2) EORAM models the graph as an array

of b^2 partitions, each is an edge block containing l secret edges. The indices of EORAM is the flattened indices of edge blocks, *i.e.*, the index of block (i, j) is $ib + j$.

The two sub-ORAMs are initialized in the following way, similarly to ORAM: 1) shuffling the graph partitions in the unit of partitions according to a random permutation π to construct ShufArr , and storing the secret permutation representation $\llbracket \vec{\pi} \rrbracket$. We refer to this procedure as ShuffleMem ; and 2) constructing the index map that translates the logical index $\llbracket i \rrbracket$ into a physical index p pointing to the target partition of ShufArr , where Arr_i and ShufMem_p refer to the same partition, *i.e.*, $p = \pi(i)$. The index map construction phase follows the same recursive procedure as ORAM (see Section 2.2). Note that only the number of partitions, not the partition size, determines the depth of GORAM indexing layer, *i.e.*, b and b^2 for VORAM and EORAM, respectively.

4.5 Partition Access

Given secret vertex or edge, we can access the target partition through the secure index layer of GORAM as follows:

1) Given the target vertex $\llbracket v \rrbracket$, we can compute the partition index $\llbracket \lceil \frac{v}{k} \rceil \rrbracket$ directly and obtain the partition containing bl secret edges by accessing VORAM. This partition contains *all* the direct neighbors of $\llbracket v \rrbracket$.

2) Given the target edge $(\llbracket v_s \rrbracket, \llbracket v_d \rrbracket)$, we can at first compute the partition index $\llbracket \lceil \frac{v_s}{k} \rceil * b + \lceil \frac{v_d}{k} \rceil \rrbracket$ and obtain the partition containing l secret edges by accessing EORAM. This partition contains *all* the edge $(\llbracket v_s \rrbracket, \llbracket v_d \rrbracket)$, if it exists in the global graph.

In summary, the partition access procedure in GORAM is almost equivalent to the ORAM access. The key difference is that GORAM obtains the target partition after getting the translated physical index p , rather than a single element.

4.6 Vectorization and Parallelization

GORAM is a *parallel-friendly* data structure. All stages in its lifecycle can be accelerated through parallel processing.

In the local process stage (Section 4.2), each data provider can independently transform the private graph G_i into the 2d-partitioned format, during which the edge blocks can be processed in parallel. Then, the computation servers integrate the N secret graphs $\{\llbracket G_i.\text{Block} \rrbracket\}_{i=1}^N$ into the secret partitioned global graph $\llbracket G.\text{Block} \rrbracket$ (Section 4.3). The primary bottleneck in this stage is the *odd_even_merge_sort* of the b^2 edge blocks, which can be performed in at most b^2 tasks in parallel. After obtaining the $b \times b \times l$ graph partition of the global graph G , we can split it into p *partition slices* for arbitrary $p \leq l$. Specifically, we split the $b \times b$ edge blocks by edges into $p \times b \times b \times l^{(j)}$ partition slices, $l = \sum_{j=1}^p l^{(j)}$. Each slice contains all the edge blocks but fewer edges per block. We can then establish p secure indices for each partition slice in parallel (Section 4.4). For each query, the p partition slices can be accessed and processed in parallel (Section 4.5). Each slice can be processed through vectorization for better performance (Section 6). The query result can be obtained by merging the results of p partition slices.

5 Initialization Optimization

During initialization, the ShuffleMem construction procedure, *i.e.*, shuffling the data according to random permutation π and storing

$S1(A, B)$	$S2(B, C)$	$S3(C, A)$
0) Construct the shares of $L = [n]$.		
$L_A = Z_1 \oplus L$	$L_B = Z_2$	$L_C = Z_3$
$\leftarrow L_A$	$\leftarrow L_B$	$\leftarrow L_C$
1) Prepare the correlated randomness.		
$Z_{12}, Z_{12}^L, \tilde{B}$ π_{12} and π_{12}^{-1}	$Z_{12}, Z_{12}^L, \tilde{B}$ π_{12} and π_{12}^{-1}	$Z_{23}, Z_{23}^L, \tilde{L}_C$ π_{23} and π_{23}^{-1}
$Z_{31}, Z_{31}^L, \tilde{A}, \tilde{L}_A$ π_{31} and π_{31}^{-1}	$Z_{23}, Z_{23}^L, \tilde{L}_C$ π_{23} and π_{23}^{-1}	$Z_{31}, Z_{31}^L, \tilde{A}, \tilde{L}_A$ π_{31} and π_{31}^{-1}
2) Main protocol: computation and communications		
$X_1 = \pi_{12}(A \oplus B \oplus Z_{12})$ $X_2 = \pi_{31}(X_1 \oplus Z_{31})$	$Y_1 = \pi_{12}(C \oplus Z_{12})$ $LY_1 = \pi_{23}^{-1}(L_B \oplus Z_{23}^L)$	$LX_1 = \pi_{23}^{-1}(L_C \oplus L_A \oplus Z_{23}^L)$ $LX_2 = \pi_{31}^{-1}(LX_1 \oplus Z_{31}^L)$
$X_2 \leftrightarrow LY_1$		$Y_1 \leftrightarrow LX_2$
$LY_2 = \pi_{31}^{-1}(LY_1 \oplus Z_{31}^L)$ $LY_3 = \pi_{12}^{-1}(LY_2 \oplus Z_{12}^L)$ $\tilde{L}_{B_1} = LY_3 \oplus \tilde{L}_A$	$X_3 = \pi_{23}(X_2 \oplus Z_{23})$ $\tilde{C}_1 = X_3 \oplus \tilde{B}$ $LX_3 = \pi_{12}^{-1}(LX_2 \oplus Z_{12}^L)$ $\tilde{L}_{B_2} = LX_3 \oplus \tilde{L}_C$	$Y_2 = \pi_{31}(Y_1 \oplus Z_{31})$ $Y_3 = \pi_{23}(Y_2 \oplus Z_{23})$ $\tilde{C}_2 = Y_3 \oplus \tilde{A}$
$L_{B_1} \leftrightarrow L_{B_2}$		$\tilde{C}_1 \leftrightarrow \tilde{C}_2$
$\tilde{L}_B = \tilde{L}_{B_1} \oplus \tilde{L}_{B_2}$	$\tilde{L}_B = \tilde{L}_{B_1} \oplus \tilde{L}_{B_2}$	$\tilde{C} = \tilde{C}_1 \oplus \tilde{C}_2$
3) Output		
$\tilde{A}, \tilde{B}, \tilde{L}_A, \tilde{L}_B$	$\tilde{B}, \tilde{C}, \tilde{L}_B, \tilde{L}_C$	$\tilde{C}, \tilde{A}, \tilde{L}_C, \tilde{L}_A$

Protocol 1: ShuffleMem Build Protocol Π_{ShufMem}

the secret permutation representation $\llbracket \vec{\pi} \rrbracket$, is the most expensive part. For Arr with n blocks and each block contains B bits, the original ShuffleMem (*i.e.*, *Waksman permutation network* adopted in [67]) incurs $O(nB \log n)$ communication and computation, which is impractical for large nB , and it becomes worse because graph introduces a series of padding elements for each block, *i.e.*, larger B . To optimize this, GORAM designs a constant-round $O(nB)$ ShuffleMem construction protocol to accelerate the initialization process.

The ShuffleMem procedure. The computation servers begin with a secret shared array $\llbracket D \rrbracket = \{\llbracket D_0 \rrbracket, \llbracket D_1 \rrbracket, \dots, \llbracket D_{n-1} \rrbracket\}$ of n partitions. At the end of the protocol, the computation servers output two secret shared arrays $\llbracket \tilde{D} \rrbracket$ and $\llbracket \vec{\pi} \rrbracket$, where \tilde{D} is a permutation of D under some random *permutation* π and $\llbracket \vec{\pi} \rrbracket$ is the secret-shared *permutation representation* of π . The permutation π is a bijection mapping from D to itself that moves the i th object D_i to place $\pi(i)$. $\tilde{D} = \{\tilde{D}_0, \tilde{D}_1, \dots, \tilde{D}_{n-1}\} = \pi(D)$, satisfies that $D_i = \tilde{D}_{\pi(i)}, \forall i \in \{0, 1, \dots, n-1\}$. $\llbracket \vec{\pi} \rrbracket = \{\llbracket \pi^{-1}(0) \rrbracket, \llbracket \pi^{-1}(1) \rrbracket, \dots, \llbracket \pi^{-1}(n-1) \rrbracket\}$ is the secret-shared permutation representation of π . Each $\vec{\pi}_i$ records the location of D_i in \tilde{D} .

Key idea of constant-round construction. For (2, 3) secret shares, Araki *et al.* [10] propose a constant-round shuffle protocol that can compute \tilde{D} in $O(n)$ complexity and $O(1)$ communication rounds. However, their protocol does not consider $\llbracket \vec{\pi} \rrbracket$. The key idea here is to extend their protocol to construct $\llbracket \vec{\pi} \rrbracket$ simultaneously by leveraging the properties of permutations:

- * Permutations are composable, *i.e.*, $\pi_1 \circ \pi_2$ is also a permutation such that $(\pi_1 \circ \pi_2)(x) = \pi_1(\pi_2(x))$ given array x .
- * Permutations are invertible, for each permutation π , there exists π^{-1} such that $(\pi^{-1} \circ \pi)(x) \equiv x$.

- * The permutation representation $\tilde{\pi} = \pi^{-1}(L)$, where $L = \{0, 1, \dots, n-1\}$, n is the size of x .

Specifically, Araki *et al.* [10] implement the random permutation by letting the computation servers collaboratively shuffle the data using three random permutations π_{12} , π_{23} and π_{31} , *i.e.*, $\tilde{D} = \pi_{23} \circ \pi_{31} \circ \pi_{12}(D) = \pi(D)$. The permutation π_{ij} is only known by servers S_i and S_j . Because each computation server only knows two of the three random permutations, the overall permutation $\pi = \pi_{23} \circ \pi_{31} \circ \pi_{12}$ remains random for each computation server. Following their structure, we can compute the corresponding secret permutation representation $[\tilde{\pi}]$ simultaneously by shuffling the ranging array $L = \{0, 1, \dots, n-1\}$ using the inverse permutations *i.e.*, $[\tilde{\pi}] = \pi^{-1}(L) = \pi_{12}^{-1} \circ \pi_{31}^{-1} \circ \pi_{23}^{-1}(L)$.

ShuffleMem construction. Protocol 1 shows the ShuffleMem construction. Each pair of computation servers S_i and S_j share a common random seed $s_{i,j}$ beforehand. As input to this protocol, computation server S_1 holds shares A, B ; S_2 holds B, C and S_3 holds C, A , satisfying that the input $D \equiv A \oplus B \oplus C$. Also, the computation servers construct the shares of the ranging array $L = \{0, 1, \dots, n-1\} \equiv L_A \oplus L_B \oplus L_C$, which requires one round of communications. Specifically, S_1, S_2 and S_3 at first hold an array of secret shares on zeros, *i.e.*, $Z_1 \oplus Z_2 \oplus Z_3 \equiv \vec{0}$, $|\vec{0}| = n$. Each Z_i is uniform random and is only known to S_i . The construction of zero secret shares requires no interactions after one-time setup [49]. S_1 locally computes $L_A = Z_1 \oplus L$ and each server sends its local share to the previous server to obtain the secret shares of L (step 0). The first step of Protocol 1 is to set up the correlated randomness using the pairwise random seed. Specifically, each pair of S_i and S_j generates randomness $Z_{i,j}, Z_{i,j}^L$, as well as randomness about their sharing shares of D and L , *i.e.*, \tilde{A}, \tilde{B} and \tilde{L}_A, \tilde{L}_C . Also, each pair of S_i and S_j generates a random permutation $\pi_{i,j}$ and the inverse permutation $\pi_{i,j}^{-1}$.

The computation servers then begin the main protocol. There are two invariants held during the protocol: 1) $X_i \oplus Y_i$ is a permutation of D and 2) $LX_i \oplus LY_i$ is an inverse permutation of L . For example, $X_1 \oplus Y_1 = \pi_{12}(A \oplus B \oplus Z_{12}) \oplus \pi_{12}(C \oplus Z_{12}) = \pi_{12}(A \oplus B \oplus C) = \pi_{12}(D)$, $LY_1 \oplus LX_1 = \pi_{23}^{-1}(L_B \oplus Z_{23}^L) \oplus \pi_{23}^{-1}(L_C \oplus L_A \oplus Z_{23}^L) = \pi_{23}^{-1}(L)$. That is, during the main protocol, the servers sequentially compute $X_1 \oplus Y_1 = \pi_{12}(D)$, $X_2 \oplus Y_2 = (\pi_{31} \circ \pi_{12})(D)$ and $X_3 \oplus Y_3 = (\pi_{23} \circ \pi_{31} \circ \pi_{12})(D)$, which constitutes the final shares of $\pi(D)$. The random permutation $\pi = \pi_{23} \circ \pi_{31} \circ \pi_{12}$. The permutation representation $\tilde{\pi} = \pi^{-1}(L) = (\pi_{12}^{-1} \circ \pi_{31}^{-1} \circ \pi_{23}^{-1})(L)$ is constructed similarly while in the reverse order.

Correctness. From the two invariants, it is straightforward to see the correctness of ShuffleMem Protocol 1. Because the final shares satisfy that $\tilde{A} \oplus \tilde{B} \oplus \tilde{C} = \tilde{X}_3 \oplus \tilde{Y}_3 = \pi(D)$, and $\tilde{L}_A \oplus \tilde{L}_B \oplus \tilde{L}_C = \tilde{L}\tilde{X}_3 \oplus \tilde{L}\tilde{Y}_3 = \pi^{-1}(L)$, the correctness is guaranteed.

Security. The security of the original shuffle protocol [10] is guaranteed by the property that each server only knows two of the three random permutations, hence the final permutation π remains random for each server. This property stands for the inverse permutation π^{-1} as well. Because Protocol 1 only extends the original shuffle [10] by applying the inverse permutation on the ranging array L , the security guarantee keeps the same with the original.

Algorithm 2: EdgeExist

Inputs : Target edge $([v_s], [v_d])$ and the target partition ID $[i] = \lceil \lceil \frac{v_s}{k} \rceil * b + \lceil \frac{v_d}{k} \rceil \rceil$.

Output : $[\text{flag}]$ indicating whether the target edge exist in global G or not.

// Partition extraction.

1 Fetch the target edge block $[B] \leftarrow \text{EORAM.access}([i])$, where $[B]$ contains l source_nodes and dest_nodes;

// Vectorized edges comparisons.

2 Construct $[\vec{v}_s]$ and $[\vec{v}_d]$ by expanding $[v_s]$ and $[v_d]$ l times;

3 Compute $[\text{mask}_s] \leftarrow \text{EQ}([\vec{v}_s], [B].\text{source_nodes})$;

4 Compute $[\text{mask}_d] \leftarrow \text{EQ}([\vec{v}_d], [B].\text{dest_nodes})$;

5 Compute $[\text{mask}] \leftarrow \text{AND}([\text{mask}_s], [\text{mask}_d])$;

// Aggregating the result through OR.

6 **while** $\text{len}([\text{mask}]) > 1$ **do**

7 Pad $[0]$ to $[\text{mask}]$ to be even ;

8 Split $[\text{mask}]$ half-by-half to $[\text{mask}]_l$ and $[\text{mask}]_r$;

9 Aggregate $[\text{mask}] \leftarrow \text{OR}([\text{mask}]_l, [\text{mask}]_r)$;

10 **end**

11 $[\text{flag}] = [\text{mask}]$;

12 **return** $[\text{flag}]$;

6 Use GORAM for Ego-centric Queries

We briefly show how to implement ego-centric queries through GORAM using five examples, which cover all the queries listed in LinkBench [39].

6.1 Basic Queries

EdgeExist is a basic query that checks whether a given edge (v_s, v_d) exists, as shown in Algorithm 2. As we analyzed in Section 4.1, if edge $(v_s, v_d) \in E$, it must be included in partition $(\lceil \frac{v_s}{k} \rceil, \lceil \frac{v_d}{k} \rceil)$. We can reduce the to-be-processed graph size to a partition of size l by accessing the EORAM using secret index $\lceil \lceil \frac{v_s}{k} \rceil * b + \lceil \frac{v_d}{k} \rceil \rceil$. Then, we compare all the edges with the given edge, the result is a secret $[\text{mask}]$ indicating which edge is equivalent to the given edge. We obtain the result by aggregating the $[\text{mask}]$ through OR.

NeighborsCount counts the number of target vertex v 's outing neighbors, as demonstrated in Algorithm 3. Because the query is about vertex v , we refer to VORAM for the corresponding partition of size bl using secret index $\lceil \lceil \frac{v}{k} \rceil \rceil$. This partition contains all the outing neighbors of v . Similarly, we obtain the result by comparing all starting vertices to v and summing up the result indicator variables. As summation is functionally equivalent to addition, we transfer the boolean shared $[\text{mask}]$ to arithmetic shares, *i.e.*, $[\text{mask}]^A$, for free communications. Note that we do not de-duplicate the neighbors because some real-world applications treat the edges between two vertices as different connections (*e.g.*, with varied timestamps [39]). For the number of unique outing neighbors, we can further de-duplicate the comparison result obviously before counting, see Appendix B.

NeighborsGet is the third basic query that extracts all the 1-hop outing neighbors of a target vertex v , while maintaining the connectivity strength (*i.e.*, how many edges) private between each neighbor and v . The implementation is outlined in Algorithm 4. The first 3 lines access the corresponding partition and compare all

Algorithm 3: NeighborsCount

Inputs : Target vertex $[[v]]$ and the target block ID $[[i]] = \lceil \frac{v}{k} \rceil$.
Output : $[[num]]^A$, the number of v 's outing neighbors.
// Partition extraction.

- 1 Fetch the target edge blocks $[[B]] \leftarrow \text{VORAM.access}([[i]])$, where $[[B]]$ contains (bl) source_nodes and dest_nodes;
// Filtering real neighbors.
- 2 Construct $[[\vec{v}]]$ by expanding $[[v]]$ bl times;
- 3 Compute $[[mask]] \leftarrow \text{EQ}([[v]], [[B]].\text{source_nodes})$;
- 4 Obtain the arith shares $[[mask]]^A \leftarrow \text{B2A}([[mask]])$;
// Counting real neighbor masks.
- 5 $[[num]]^A \leftarrow \text{SUM}([[mask]]^A)$;
- 6 **return** $[[num]]^A$;

Algorithm 4: NeighborsGet

Inputs : Target vertex $[[v]]$ and the target block ID $[[i]] = \lceil \frac{v}{k} \rceil$.
Output : $[[neighbors]]$, containing the unique outing neighbor's IDs of $[[v]]$.
// Partition extraction.

- 1 Fetch the target edge blocks $[[B]] \leftarrow \text{VORAM.access}([[i]])$, where $[[B]]$ contains (bl) source_nodes and dest_nodes;
// 1) Filtering real neighbors.
- 2 Construct $[[\vec{v}]]$ by expanding $[[v]]$ bl times;
- 3 Compute $[[mask]] \leftarrow \text{EQ}([[v]], [[B]].\text{source_nodes})$;
// 3) Obtaining the neighbors and masking the others out.
- 4 Compute $[[candidate]] \leftarrow \text{MUL}([[mask]], [[B]].\text{dest_nodes})$;
// 4) De-duplicating neighbors.
- 5 $[[same_mask]] \leftarrow \text{NEQ}([[candidate]]_{[1]}, [[candidate]]_{[-1]})$;
- 6 $[[same_mask]].\text{append}([1])$;
- 7 $[[neighbors]] \leftarrow \text{MUL}([[same_mask]], [[candidate]])$;
// 5) Shuffling the neighbors.
- 8 $[[neighbors]] \leftarrow \text{SHUFFLE}([[neighbors]])$;
- 9 **return** $[[neighbors]]$;

the starting vertices with the target v to construct $[[mask]]$, which indicates the edges started from v . Then, we multiply the $[[mask]]$ and the destination vertices to obtain the $[[candidate]]$, where each element is $[[0]]$ or $[[u]]$ if u is an outing neighbor of v . Note that the number of $[[u]]$ implies the connectivity strength between u and v , therefore we de-duplicate $[[candidate]]$ in lines 5-8 to mask out this information. Because each partition is sorted by key $v||u$ in the integration stage (see Section 4.3), all the same outing neighbors in $[[candidate]]$ are located successively as a group. We apply the NEQ on $[[candidate]]$ differentially for $[[same_mask]]$. Only the last outing neighbor $[[u]]$ in each group is $[[1]]$, while the rest are $[[0]]$. By multiplying $[[same_mask]]$ and $[[candidate]]$, the duplicate neighbors are masked as $[[0]]$. Note that the gap between two successive neighbors u_i, u_{i+1} implies how many u_{i+1} exist, therefore we apply the SHUFFLE to permute this location-implied information before returning to the client.

6.2 Complex queries

The clients can fulfill more complicated queries by submitting multiple basic queries introduced above. Also, the client can provide

Table 1: Synthetic Graphs

Graph Types	Generation Methods	Average Degree
k_regular	K_Regular [1]	7.5
bipartite	Random_Bipartite [2]	134.4
random	Erdos_Renyi [3]	268.8
powerlaw	Barabasi [4]	523.7
geometric	GRG [5]	1198.5

user-defined functions for arbitrary statistic queries. We use two examples to demonstrate the usages.

Cycle-identification plays a crucial role in transaction graph analysis. Identifying whether the transactions across multiple suspicious accounts form a cycle is an effective way for money laundering detection [45, 53]. Cycle identification can be achieved by submitting a series of EdgeExist queries. For example, given three vertices v_1, v_2 and v_3 , by submitting EdgeExist queries on edges $(v_1, v_2), (v_2, v_3), (v_3, v_1)$ and their reverse edges, the client can detect whether a cycle exists among the three vertices. Similarly, the clients can submit more EdgeExist queries for more vertices.

Statistic queries. Also, the client can express arbitrary ego-centric statistic queries on graphs with properties, *i.e.*, each edge has extra fields recording the properties like creation timestamp and transaction amounts. These queries can be simply implemented by augmenting the process of the basic queries. For instance, to perform *association range queries* [39], which count the outing edges created before a provided timestamp, the client can add an extra comparison in NeighborsCount to compute whether the creation timestamp is less than the given timestamp before counting the result. Specifically, the client can compute $[[t_mask]] \leftarrow \text{LT}([[timestamp\ field]], [[given\ threshold]])$ and update the neighbors mask in the 3rd line to $[[mask]] = \text{AND}([[mask]], [[t_mask]])$. The final result, $[[num]]^A$, is now the number of outing edges created before the given timestamp. Similarly, the client can implement arbitrary ego-centric analysis by providing user-defined functions.

7 Evaluation

7.1 Evaluation Setup

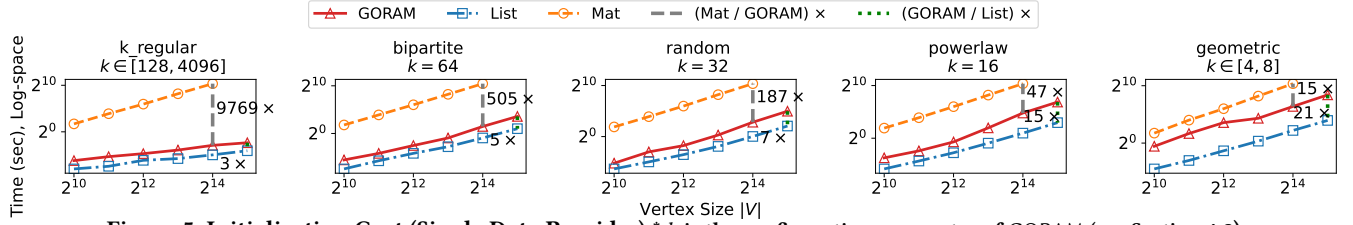
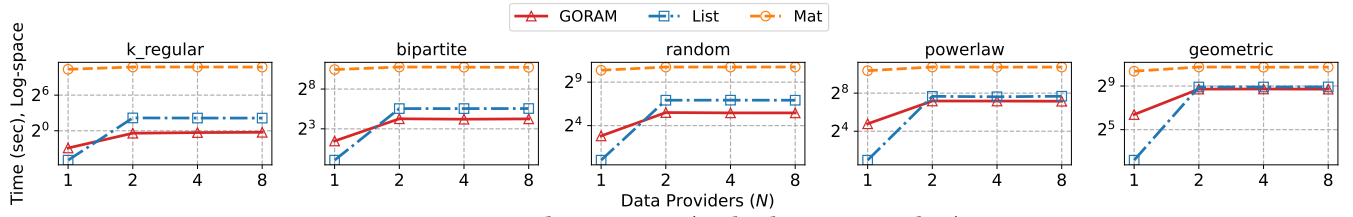
Setup. We implement a prototype querying engine by integrating GORAM on the widely adopted 3-party MPC platform, ABY3 [49]. All the following evaluations are run on a cluster of three computation servers, each equipped with 16 CPU cores and 512GB memory. The underlying hardware consists of Intel(R) Xeon(R) Gold 6330 CPU@2.00GHz, and is connected via a 10Gbps full duplex link, with an average round-trip-time (RTT) of 0.12ms.

Graph types and queries. We adopt two sets of graphs and five different graph queries to benchmark the performance of GORAM. The two sets of graphs include: 1) Five classes of synthetic graphs, with each class containing six different scale graphs. The vertices of these graphs scale from 1K to 32K, and the edges are generated according to the given distribution through igraph [29]. Table 1 summarizes the generation methods and the average degrees of each class, *i.e.*, averaged from six scale graphs. 2) Three real-world graphs, Slashdot [6], DBLP [65] and Twitter [17]. The sizes range from less than 1 million to more than 1 billion edges. Detailed

Table 2: Complexity Overview

Data Structures		Initialization		Partition Access		Partition Processing for Basic Queries					
						EdgeExist		NeighborsCount		NeighborsGet	
		Comp	Round	Comp	Round	Comp	Round	Comp	Round	Comp	Round
<i>Mat</i>	adj-VORAM	$O(N V ^2)$	$3 + 2\log_p(\frac{ V }{T})$	$O(PT \log_p(\frac{ V }{T}))$	$O(\log_p(\frac{ V }{T}))$	$O(1)$	$O(1)$	$O(V)$	$O(1)$	$O(V)$	$O(1)$
	adj-EORAM		$3 + 2\log_p(\frac{ V ^2}{T})$	$O(PT \log_p(\frac{ V ^2}{T}))$	$O(\log_p(\frac{ V ^2}{T}))$						
<i>List</i>		$O(E \log(E) \log(N))$	$\log(E) \log(N)$	$O(1)$	NA	$O(E)$	$O(\log(E))$	$O(E)$	$O(1)$	$O(E)$	$O(1)$
GORAM	VORAM	$O(b^2 l \log(l) \log(N)), N > 1$ Or $O(b^2 l)$ when $N = 1$	$3 + \log(l) \log(N) + 2\log_p(\frac{b}{T})$	$O(PT \log_p(\frac{b}{T}))$	$O(\log_p(\frac{b}{T}))$	$O(l)$	$O(\log(l))$	$O(bl)$	$O(1)$	$O(bl)$	$O(1)$
	EORAM		$3 + \log(l) \log(N) + 2\log_p(\frac{b^2}{T})$	$O(PT \log_p(\frac{b^2}{T}))$	$O(\log_p(\frac{b^2}{T}))$						

P and T denote the pack and stash size of ORAM, and b, l are the configuration parameters of 2d-partition, where $b = \frac{|V|}{k}$. The Round complexities with the $O(\cdot)$ notation is in the unit of EQ, and the Partition Access complexities are the averaged complexity of successive T queries. N is the number of data providers, $N \geq 1$.

**Figure 5: Initialization Cost (Single Data Provider)** * k is the configuration parameter of GORAM (see Section 4.3)**Figure 6: Initialization Cost (Multiple Data Providers)**

information is presented in Section 7.4. For queries, we use three basic queries and two complex queries illustrated in Section 6.

7.2 Strawman Solutions

We construct two sets of baselines to evaluate GORAM by implementing queries on the strawman data structures: adjacency matrix (*Mat*) and edge list (*List*), as detailed in Section 3.2

Basic queries using *Mat*. Using the *Mat* data structure, we can implement the three basic queries as follows: For 1) *EdgeExist* query on edge (v_i, v_j) , we can determine its existence by directly extracting the element (i, j) from the adj-EORAM (see Section 3.2) and comparing it to 0; for 2) *NeighborsCount*, we refer to adj-VORAM and sum up the edge numbers; and for 3) *NeighborsGet*, we refer to adj-VORAM, compare the elements with 0 through GT to eliminate the connectivity strengths, and then return the result to the client.

Basic queries using *List*. Using *List* data structure, we can implement the three basic queries by scanning the whole edge list, akin to GORAM's procedure of processing each partition while on the whole *List*.

7.3 Comparison with Strawman Solutions

We compare GORAM with the two strawman solutions using the synthetic graphs, demonstrating the superiority of GORAM data

structure across varied graph sizes and distributions. All the reported times represent the wall-clock time averaged from 5 runs. For GORAM and *Mat* that require ORAM accesses, the time is the averaged time of successive T queries, where T is the stash size³ and $T = \sqrt{\#(\text{items in ORAM})}$, the default setting in [67]. Because *Mat* is non-trivial to parallelize, all evaluations in this section are run using a single thread. The complexity of each stage is summarized in Table 2, and the performance results (Figure 5 to 7) are presented according to the sparsity of the graphs, *i.e.*, the leftmost *k_regular* is the sparsest graph with 7.5 average degree, and the rightmost *geometric* is the densest graph, with 1198.5 average degree.

Initialization. Figure 5 shows the initialization cost when there is only one data provider, the cost is the wall-clock time from data loading to secure indices construction (affecting only GORAM and *Mat*, *List* does not require establishing indices). Figure 6 presents the cost when there are multiple data providers (1 to 8). We simulate the distributed graphs by randomly assigning each edge of the synthetic graph with 16K vertices to each data provider, which is the largest scale supported by *Mat*. A full evaluation on varied scales is shown in Appendix C. We observe:

³Because we only support static queries, we can always initialize fresh ORAMs in background processes. When the stash is full, we can directly process queries using a fresh ORAM without waiting.

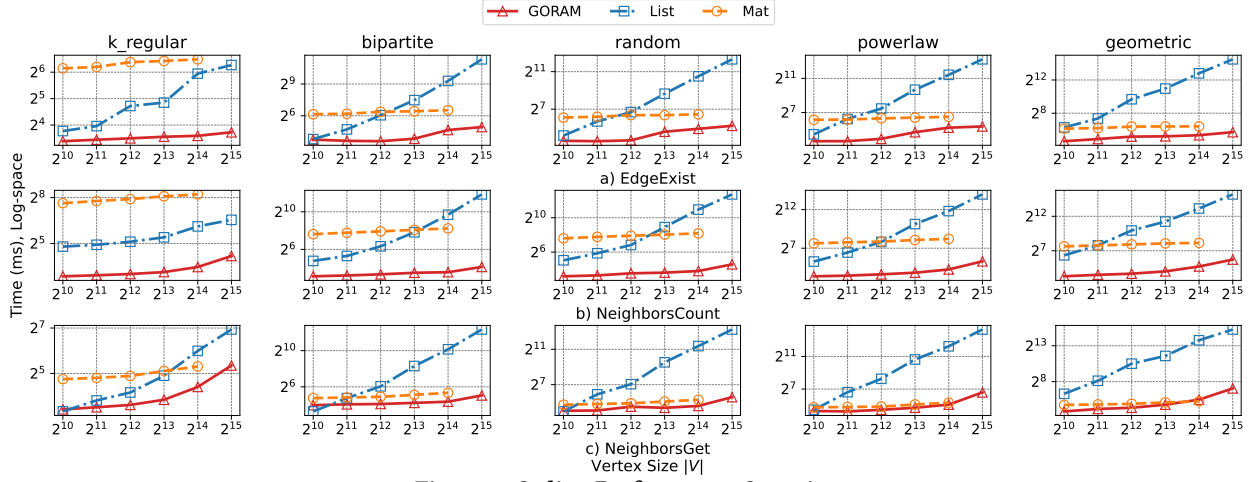


Figure 7: Online Performance Overview

Table 3: Parameters of Synthetic Graphs with $|V| = 2^{15}$

Graph Type	$ E $	b	l	bl	$b^2l/ E $
k_regular	0.2M	8	4001	32.0K	1.04
bipartite	13.4M	512	87	44.5K	1.70
random	26.8M	1024	56	57.3K	2.19
powerlaw	52.3M	2048	48	98.3K	3.85
geometric	105.0M	4096	32	131.0K	5.11

The parameters b and l refer to the vertex group numbers and the edge block size with padded edges, see Section 4.1. l is the EORAM partition size, bl is the VORAM partition size.

1) *Single data provider.* As Table 2 shows, the initialization cost is linear to the graph sizes, *i.e.*, $|V|^2$ or $|E|$. GORAM and *List* contain an extra log factor due to the merge sort stage, which is unnecessary when there is one data provider. Given the relationship $|E| < b^2l < |V|^2$ among *List*, GORAM, and *Mat*, the initialization costs follow the order: $Mat > GORAM > List$, as shown in Figure 5. Also, *Mat* has the highest, and constant cost for both sparse and dense graphs.

2) *Multiple data providers.* For N data providers, both GORAM and *List* need to perform the merge sort on N ordered private graphs during the initialization (see Section 4.3). When $N > 1$, the initialization cost of GORAM becomes more efficient than that of *List* for all graphs with 16K vertices. This is because GORAM can merge all b^2 edge blocks (each with length l) in a single sorting pass for every two data providers, making the depth of GORAM $\log(l) \log(N)$. In contrast, the sorting depth of *List* is $\log(|E|) \log(N)$, and $|E| \gg l$ for most cases, see Table 3. Once $N > 1$, GORAM performs better than *List*, particularly for sparse graphs. For dense graphs, the higher total work, *i.e.*, $b^2l > |E|$, offsets the savings from the smaller depth.

3) *Scale to large and sparse graphs.* By avoiding the dependence on the factor of $|V|$, GORAM effectively scales to large yet sparse graphs, which is exactly the case of most real-world graphs [6, 17, 65]. As a comparison, *Mat* runs out of memory during the construction of adj-EORAM on all graphs with 32K vertices even with 512GB memory because of the $O(|V|^2)$ space complexity.

Query Processing. Figure 7 presents the time processing three basic queries using GORAM, *Mat*, and *List*. Each time represents the

duration from partition access to the completion of query processing. We can see that GORAM delivers highly efficient query response across all 90 test cases (6 sizes, 5 graph types, and 3 queries). On average, GORAM completes all basic queries in 22.0 ms. The slowest query is the NeighborsGet on the largest geometric graph, which takes 132.8 ms, satisfying the efficiency requirement in Section 3.

1) *Compared to Mat*, which requires a complexity of $O(\log(|V|))$ to access the target row or element in the adjacency matrix for each query, and up to $O(|V|)$ time to process NeighborsCount and NeighborsGet, GORAM is more efficient, particularly for sparse graphs like k_regular. GORAM only constructs indices for each partition, thereby reducing the cost for accessing the target partition to $O(\log b)$. Despite sometimes having higher partition processing complexity, *e.g.*, $O(l)$ vs. $O(1)$ for EdgeExist, GORAM achieves significant advantages for sparse graphs. For instance, GORAM achieves an average speedup of 9.4 \times and a maximum speedup of 30.7 \times on NeighborsCount for the 2^{13} vertices k_regular graph.

2) *Compared to List* that scans the entire edge list E for each query, GORAM reduces the to-be-processed graph size effectively. Because both the EORAM and VORAM partition sizes l and $bl \ll |E|$, shown in Table 3, GORAM achieves significant performance improvements, with an average speedup of 67.6 \times . The speedups become more remarkable for denser graphs. Specifically, GORAM presents 703.6 \times speedup on the densest geometric graph.

Adaptivity. As Table 2 shows, the performance of *Mat* and *List* is directly related to the vertex numbers $|V|$ or the edge numbers $|E|$. This makes them suitable for either excessively dense or sparse graphs. For example, *Mat* performs well on the densest geometric graph while degrading on the sparsest k_regular. *List*, conversely, performs better on sparse graphs. As a comparison, GORAM demonstrates adaptability by adjusting the configuration parameter k to fit for various distributed graphs. We can see from Figure 5, the auto-configured parameter k decreases as the graph density increases. k determines the number of vertices per chunk and the chunk number $b = \frac{|V|}{k}$. Smaller k results in more chunks and smaller partition sizes. Specifically, $k \in [128, 4096]$ for k_regular, and decreases for denser graphs till $k \in [4, 8]$ for geometric.

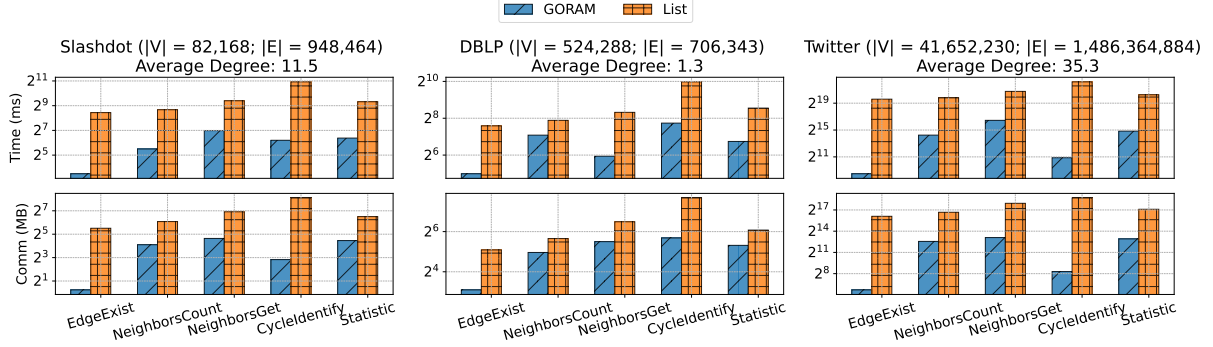


Figure 8: Queries on Real-world Graphs (* the y-axes are in log-scale.)

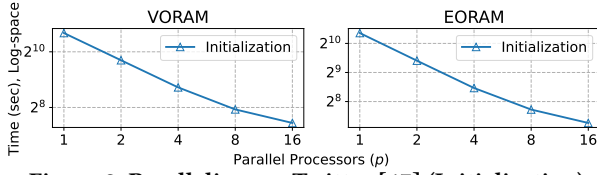


Figure 9: Parallelism on Twitter [17] (Initialization)

7.4 Performance on Real-world Graphs

In this section, we analyze the performance and communications of both basic and complex queries introduced in Section 6 on three real-world graphs. These graphs are ordered by the graph vertex numbers, and the sizes are shown in Figure 8. Specifically, the largest Twitter [17] graph contains 1.4 billion edges. Note that we do not include *Mat* in the following evaluation because it runs out of memory for all real-world graphs.

Performance of the five queries is shown in the first line of Figure 8. For smaller graphs Slashdot [6] and DBLP [65], GORAM completes all the queries in 135.7 ms. For the largest Twitter, GORAM can accelerate its performance through parallelization, as analyzed in Section 7.5. Compared to the strawman solutions, GORAM achieves significant benefits in scalability and efficiency. Compared to *Mat*, GORAM can construct query engines for extremely large graphs, e.g., Twitter with more than 41M vertices. Compared to *List*, GORAM achieves notable performance improvements, especially on the largest graph. The average speedup across all the three graphs using a single processor is 278.2 \times . On the largest Twitter, GORAM achieves a remarkable speedup of 812.5 \times . Notably, GORAM achieves more significant speedups for the two edge-centric queries, i.e., *EdgeExist* and *CycleIdentify*, with 2215.6 \times and 2527.5 \times speedups, respectively. This is because GORAM splits the graph into b^2 partitions for edge-centric queries (and b for vertex-centric), leading to smaller partition size and consequently better performance.

Communications. The bottom line in Figure 8 shows the communication costs. Specifically, the average bytes sent by each computation server. As can be seen, GORAM significantly reduces the communications compared to *List*, achieving an average savings, calculated as $(1 - \frac{\text{Comm}(\text{GORAM})}{\text{Comm}(\text{List})})$, of 78.4%. The maximum savings, remarkable 99.9%, are observed in *EdgeExist* and *CycleIdentify* queries on Twitter. This is because GORAM splits the graph into b^2 partitions (for Twitter, $b^2 = 4096$), and processes only one partition

for each query, thereby significantly reducing online communications. The savings for the other vertex-centric queries, where the graph is split into b partitions instead of b^2 , tend to be relatively smaller but still significant, with an average saving of 72.3%. The communication savings align with the speedups shown in the first line of Figure 8.

7.5 Parallelization for Large-scale Graph

As introduced in Section 4.6, both the initialization and the query processing stages of GORAM can be accelerated through multiple processors. We evaluate the scalability of GORAM on the largest Twitter graph, using 1-16 processors.

Initialization. Figure 9 shows the parallel initialization cost. Specifically, we split the $b \times b \times l$ 2d-partitioned global graph into p $b \times b \times l^{(j)}$, $j \in [p]$ smaller graphs and then build p GORAM in parallel. By leveraging $p = 16$ processes, we can construct both VORAM and EORAM for the billion-edge-scale graph within 2.9 minutes. This achieves a speedup of 9.4 \times compared to the sequential construction. We can not achieve the optimal $p \times$ speedup because 10Gbps bandwidth limits the cross-party communications.

Query processing. Figure 10 shows the parallel query processing performance. Using 16 processes, GORAM finishes all the five queries on Twitter efficiently. *NeighborsGet* costs the longest 35.7 sec. The fastest *EdgeExist* only costs 58.1 ms, demonstrating the real-time query processing capability of GORAM. As can be seen, all the queries except *NeighborsGet* achieve linear scalability. *NeighborsGet* fails to achieve linear scalability because its aggregation stage across partition slices includes a non-parallelizable SHUFFLE procedure on the whole partition, which is used to mask out the connectivity strengths, i.e., the 8th line in Algorithm 4.

7.6 ShuffleMem Construction Comparison

Figure 11 compares the cost of ShuffleMem construction using *Waksman* permutation network, as adopted in [67], and our optimized constant-round ShuffleMem protocol, see Section 5. The ShuffleMem construction is the main bottleneck of building ORAM. We can see that GORAM significantly improves both computation time and communication, achieving 17.4 \times to 83.5 \times speedups and 97.5% to 98.8% communication savings as input sizes increase. This is because our method reduces the original $O(n \log(n))$ computation and communication to $O(n)$, thereby showing better performance as input sizes increase. Furthermore, unlike Waksman network,

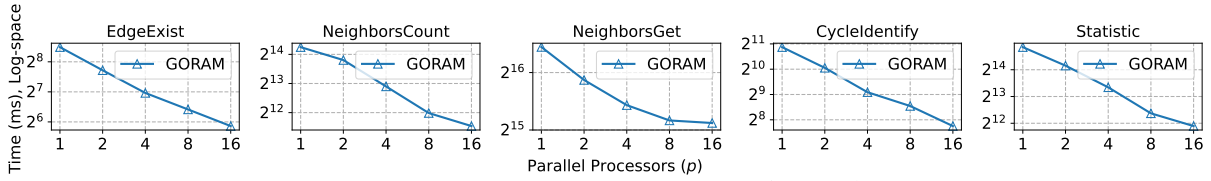


Figure 10: Parallelism on Twitter [17] (Queries)

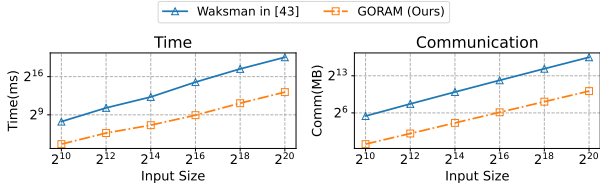


Figure 11: ShuffleMem Construction (* the y-axes are in log-scale.)

which necessitates an expensive switch operation, amounting to approximately $\approx 6n$ communications per layer in the $2 \log(n)$ depth network, GORAM only requires shares transmission and XOR operations.

8 Related Works

We discuss the prior arts related to GORAM on federated queries, secure graph processing, and distributed ORAM implementations. **Secure federated database**, initialized by SMCQL [12], focuses on conducting *public* SQL queries over the union of databases from mutually distrustful data providers while preserving privacy about the individual tuples. For each SQL query, SMCQL analyzes the statements, identifies the required data from each data provider and translates the query into secure computation protocols. Then, the involved data providers encrypt the corresponding data and run the secure protocols collaboratively to obtain the query result, during which the input data and all the intermediate results remain private. Several strategies have been proposed to enhance the practical performance of SMCQL, including Shrinkwrap [13], Conclave [59] and SAQE [14], which trade off privacy and accuracy. Recently, Secrecy [40] provides an efficient solution without compromising privacy guarantees, achieving seconds-level SELECT on 1K input tuples. Based on the above progress, Aljuaid *et al.* [8, 9] propose to process federated graph queries by directly translating the graph queries into SQL queries through [32]. We can not apply the above methods to our problem because they are all designed for *public* queries. In our settings, the query keys are expected to remain private. There are also studies focusing on secure databases with only one data provider [30, 52, 56, 63], and specialized relational operators, like JOIN [11, 37].

Secure graph data structures. As we introduced in Section 1, there are two classic data structures used for secure graph processing, *i.e.*, adjacency matrix (*Mat*) [15] and vertex-edge lists (*List*) [10, 46, 47, 51], and we adopt these two data structures as baselines. Beyond the above data structures, there are also proposals leveraging *Structured Encryption (SE)* [21] to create secure graph databases. They focus on encrypting the graph in a way that can be privately queried using a set of predefined queries [26, 38, 48, 62]. However, the SE-based methods have limitations. They are only

applicable when a *single* client wishes to outsource her graph to an untrusted server and query the graph at the same time in a way that the server can not tell her target query key. These methods rely on the fact that the one who encrypts the graph and the one who obtains the result must have the same secret key. Consequently, these methods cannot be directly extended to support multiple data providers, nor can they handle cases where the client submitting queries is not the data provider.

Graph processing under other security settings. Mazloom *et al.* [46, 47] propose to perform graph analysis guaranteeing *differential privacy (DP)* on two neighboring graphs, *i.e.*, two graphs differ on one vertex degree. Similarly, special graph algorithm, *e.g.*, *k*-star and triangle counts [31, 33?], egocentric betweenness analysis [55], sub-graph counting [61], pattern matching [60] are proposed on DP. It is worth noting that the DP definitions are not suitable in our case, as it failed to protect crucial graph distribution information of data providers, which can lead to severe privacy leakages in the real world, *e.g.*, revealing the (almost) accurate transaction amounts of certain accounts. Also, there are proposals leveraging TEEs for graph processing, like [19, 20, 64], which assumes trusted hardware and is vulnerable to side-channel attacks [43, 50]. GORAM, however, is based on MPC and provides theoretically guaranteed privacy.

DORAM implementations. There are several efficient DORAM designs. FLORAM [25] and DuORAM [58] focus on building DORAM protocols for high-latency and low-bandwidth settings, which trade a linear computation complexity for reduced communications, therefore becoming impractical for large-scale data. 3PC-DORAM [18], GigaORAM [25], and Square-root ORAM [67], on the other hand, struggle for sub-linear access complexity. GigaORAM and 3PC-DORAM depend on the *Shared-In Shared-Out Pseudo Random Functions (SISO-PRF)* to improve complexity. However, the SISO-PRF becomes practical only with efficient “MPC friendly” block ciphers, *i.e.*, LowMC [7] as they adopted, which was unfortunately cryptanalyzed [41]. GORAM builds its indexing layer drawing on the structure of the classic Square-root ORAM (Section 4.4) because it achieves sub-linear complexity and circumvents the reliance on any specific ciphers that may potentially degrade security.

9 Conclusion and Future Work

We propose GORAM, the first step towards achieving efficient private ego-centric queries on federated graphs. GORAM introduces a methodology for reducing the to-be-processed data sizes in secure computations, which relies on query-specific strategical data partitioning and secure index construction. We hope this method can be generalized to other applications beyond ego-centric queries. Extensive evaluations validate that GORAM achieves practical performance on real-world graphs, even with 1.4 billion edges. For

future work, we are going to extend GORAM to support other graph queries, such as path filtering and sub-graph pattern matching, and further optimize its performance and scalability.

References

- [1] 2006. https://igraph.org/python/api/0.9.11/igraph._igraph.GraphBase.html#K_Regular
- [2] 2006. https://igraph.org/python/api/0.9.11/igraph.Graph.html#Random_Bipartite
- [3] 2006. https://igraph.org/python/api/0.9.11/igraph._igraph.GraphBase.html#Erdos_Renyi
- [4] 2006. https://igraph.org/python/api/0.9.11/igraph._igraph.GraphBase.html#Barabasi
- [5] 2006. https://igraph.org/python/api/0.9.11/igraph._igraph.GraphBase.html#_GRG
- [6] 2009. Community Structure in Large Networks: Natural Cluster Sizes and the Absence of Large Well-Defined Clusters. *Internet Mathematics* (2009).
- [7] Martin R Albrecht, Christian Rechberger, Thomas Schneider, Tyge Tjessen, and Michael Zohner. 2015. Ciphers for MPC and FHE. In *Advances in Annual International Conference on the Theory and Applications of Cryptographic Techniques (EUROCRYPT)*. Springer.
- [8] Nouf Aljuaid, Alexei Lisitsa, and Sven Schewe. [n. d.]. Efficient and Secure Multiparty Querying over Federated Graph Databases. ([n. d.]).
- [9] Nouf Aljuaid, Alexei Lisitsa, and Sven Schewe. 2023. Secure Joint Querying Over Federated Graph Databases Utilising SMPCC Protocols. In *ICISSP*. 210–217.
- [10] Toshinori Araki, Jun Furukawa, Kazuma Ohara, Benny Pinkas, Hanan Rosemarin, and Hikaru Tsuchida. 2021. Secure Graph Analysis at Scale. In *Proceedings of the ACM SIGSAC Conference on Computer and Communications Security (CCS)*.
- [11] Gilad Asharov, Koki Hamada, Ryo Kikuchi, Ariel Nof, Benny Pinkas, and Junichi Tomida. 2023. Secure Statistical Analysis on Multiple Datasets: Join and Group-By. In *Proceedings of the ACM SIGSAC Conference on Computer and Communications Security (CCS)*.
- [12] Johes Bater, Gregory Elliott, Craig Eggen, Satyender Goel, Abel N Kho, and Jennie Rogers. 2017. SMCQL: Secure Query Processing for Private Data Networks. *Proceedings of the VLDB Endowment* (2017).
- [13] Johes Bater, Xi He, William Ehrlich, Ashwin Machanavajjhala, and Jennie Rogers. 2018. Shrinkwrap: efficient sql query processing in differentially private data federations. *Proceedings of the VLDB Endowment* (2018).
- [14] Johes Bater, Yongjoo Park, Xi He, Xiao Wang, and Jennie Rogers. 2020. SAQE: Practical Privacy-preserving Approximate Query Processing for Data Federations. *Proceedings of the VLDB Endowment* (2020).
- [15] Marina Blanton, Aaron Steele, and Mehrdad Alisagari. 2013. Data-oblivious Graph Algorithms for Secure Computation and Outsourcing. In *Proceedings of the ACM SIGSAC Symposium on Information, Computer and Communications Security (ASIA-CCS)*.
- [16] Dan Bogdanov, Sven Laur, and Jan Willemsen. 2008. Sharemind: A Framework for Fast Privacy-preserving Computations. In *European Symposium on Research in Computer Security (ESORICS)*. Springer.
- [17] Paolo Boldi and Sebastiano Vigna. 2004. The Webgraph Framework I: Compression Techniques. In *Proceedings of the International Conference on World Wide Web (WWW)*.
- [18] Paul Bunn, Jonathan Katz, Eyal Kushilevitz, and Rafail Ostrovsky. 2020. Efficient 3-party distributed ORAM. In *Security and Cryptography for Networks (SCN)*. Springer.
- [19] Javad Ghareh Chamani, Ioannis Demertzis, Dimitrios Papadopoulos, Charalampos Papamanthou, and Rasool Jalili. 2024. GraphOS: Towards Oblivious Graph Processing. *Proceedings of the VLDB Endowment* (2024).
- [20] Zhao Chang, Lei Zou, and Feifei Li. 2016. Privacy preserving subgraph matching on large graphs in cloud. In *Proceedings of the International Conference on Management of Data (SIGMOD)*.
- [21] Melissa Chase and Seny Kamara. 2010. Structured Encryption and Controlled Disclosure. In *International Conference on the Theory and Application of Cryptology and Information Security (ASIACRYPT)*. Springer.
- [22] Fan Chung. 2010. Graph Theory in the Information Age. *Notices of the AMS* (2010).
- [23] Daniel Demmler, Thomas Schneider, and Michael Zohner. 2015. ABY-A framework for Efficient Mixed-protocol Secure Two-party Computation.. In *The Network and Distributed System Security Symposium (NDSS)*.
- [24] Jack Doerner and Abhi Shelat. 2017. Scaling ORAM for Secure Computation. In *Proceedings of the ACM SIGSAC Conference on Computer and Communications Security (CCS)*.
- [25] Brett Falk, Rafail Ostrovsky, Matan Shtepel, and Jacob Zhang. 2023. GigaDORAM: breaking the billion address barrier. In *Proceedings of the USENIX Conference on Security Symposium (USENIX Security)*.
- [26] Francesca Falzon, Esha Ghosh, Kenneth G Paterson, and Roberto Tamassia. 2024. PathGES: An Efficient and Secure Graph Encryption Scheme for Shortest Path Queries. *Proceedings of the ACM SIGSAC Conference on Computer and Communications Security (CCS)* (2024).
- [27] Oded Goldreich and Rafail Ostrovsky. 1996. Software Protection and Simulation on Oblivious RAMs. *Journal of the ACM (JACM)* (1996).
- [28] Kanav Gupta, Deepak Kumaraswamy, Nishanth Chandran, and Divya Gupta. 2022. LLAMA: A Low Latency Math Library for Secure Inference. *Proceedings on Privacy Enhancing Technologies (PoPETs)* (2022).
- [29] Tamás Nepusz Gábor Csárdi. 2006. The igraph Software Package for Complex Network Research. *InterJournal Complex Systems* (2006).
- [30] Zhian He, Wai Kit Wong, Ben Kao, David Wai Lok Cheung, Rongbin Li, Siu Ming Yiu, and Eric Lo. 2015. SDB: A Secure Query Processing System with Data Interoperability. *Proceedings of the VLDB Endowment* (2015).
- [31] Jacob Imola, Takao Murakami, and Kamalika Chaudhuri. 2021. Locally Differentially Private Analysis of Graph Statistics. In *30th USENIX security symposium (USENIX Security)*.
- [32] Alekh Jindal, Prayna Rawlani, Eugene Wu, Samuel Madden, Amol Deshpande, and Mike Stonebraker. 2014. Vertexica: Your Relational Friend for Graph Analytics! *Proceedings of the VLDB Endowment* (2014).
- [33] Vishesh Karwa, Sofya Raskhodnikova, Adam Smith, and Grigory Yaroslavtsev. 2011. Private Analysis of Graph Structure. *Proceedings of the VLDB Endowment* (2011).
- [34] Marcel Keller. 2020. MP-SPDZ: A Versatile Framework for Multi-party Computation. In *ACM SIGSAC Conference on Computer and Communications Security (CCS)*.
- [35] Marcel Keller and Ke Sun. 2022. Secure Quantized Training for Deep Learning. In *International Conference on Machine Learning (ICML)*. PMLR.
- [36] Donald E Knuth. 1973. The Art of Computer Programming, VOL. 3: Searching and sorting (the Odd Even Mergesort Network Section). *Reading MA: Addison-Wisley* (1973), 543–583.
- [37] Simeon Krastnikov, Florian Kerschbaum, and Douglas Stebila. [n. d.]. Efficient Oblivious Database Joins. *Proceedings of the VLDB Endowment* 11 ([n. d.]).
- [38] Shangqi Lai, Xingliang Yuan, Shi-Feng Sun, Joseph K Liu, Yuhong Liu, and Dongxi Liu. 2019. GraphSE²: An Encrypted Graph Database for Privacy-preserving Social Search. In *Proceedings of the 2019 ACM Asia conference on computer and communications security (ASIACCS)*.
- [39] Bob Lantz, Brandon Heller, and Nick McKeown. 2010. LinkBench: a Database Benchmark based on the Facebook Social Graph. In *Proceedings of the ACM SIGCOMM Workshop on Hot Topics in Networks*. 1–6.
- [40] John Liagouris, Vasiliki Kalavri, Muhammad Faisal, and Mayank Varia. 2023. SECURE: Secure Collaborative Analytics in Untrusted Clouds. In *USENIX Symposium on Networked Systems Design and Implementation (NSDI)*.
- [41] Fukang Liu, Takanori Isobe, and Willi Meier. 2021. Cryptanalysis of Full LowMC and LowMC-M with Algebraic Techniques. In *Advances in Annual International Cryptology Conference (CRYPTO)*. Springer.
- [42] Kunlong Liu and Trinabh Gupta. 2024. Making Privacy-preserving Federated Graph Analytics with Strong Guarantees Practical (for Certain Queries). *arXiv preprint arXiv:2404.01619* (2024).
- [43] Xiaoxuan Lou, Tianwei Zhang, Jun Jiang, and Yinqian Zhang. 2021. A Survey of Microarchitectural Side-channel Vulnerabilities, Attacks, and Defenses in Cryptography. *ACM Computing Surveys (CSUR)* (2021).
- [44] Steve Lu and Rafail Ostrovsky. 2013. Distributed Oblivious RAM for Secure Two-party Computation. In *Theory of Cryptography Conference (TCC)*. Springer.
- [45] Nav Mathur. 2021. Graph Technology for Financial Services. Neo4j. <https://go.neo4j.com/rs/710-RRC-335/images/Neo4j-in-Financial%20Services-white-paper.pdf> (White Paper).
- [46] Sahar Mazloom and S Dov Gordon. 2018. Secure Computation with Differentially Private Access Patterns. In *Proceedings of the ACM SIGSAC Conference on Computer and Communications Security (CCS)*.
- [47] Sahar Mazloom, Phi Hung Le, Samuel Ranellucci, and S Dov Gordon. 2020. Secure Parallel Computation on National Scale Volumes of Data. In *USENIX Security Symposium (USENIX Security)*.
- [48] Xianrui Meng, Seny Kamara, Kobbi Nissim, and George Kollios. 2015. GRECS: Graph Encryption for Approximate Shortest Distance Queries. In *Proceedings of the ACM SIGSAC Conference on Computer and Communications Security (CCS)*. 504–517.
- [49] Payman Mohassel and Peter Rindal. 2018. ABY3: A Mixed Protocol Framework for Machine Learning. In *ACM SIGSAC conference on computer and communications security (CCS)*.
- [50] Antonio Muñoz, Ruben Rios, Rodrigo Román, and Javier López. 2023. A survey on the (in) security of trusted execution environments. *Computers & Security* (2023).
- [51] Kartik Nayak, Xiao Shaun Wang, Stratis Ioannidis, Udi Weinsberg, Nina Taft, and Elaine Shi. 2015. GraphSC: Parallel Secure Computation Made Easy. In *IEEE symposium on security and privacy (S&P)*. IEEE.
- [52] Raluca Ada Popa, Catherine MS Redfield, Nickolai Zeldovich, and Hari Balakrishnan. 2011. CryptDB: Protecting Confidentiality with Encrypted Query Processing. In *Proceedings of the ACM Symposium on Operating Systems Principles (SOSP)*.

- [53] Xiafei Qiu, Wubin Cen, Zhengping Qian, You Peng, Ying Zhang, Xuemin Lin, and Jingren Zhou. 2018. Real-time Constrained Cycle Detection in Large Dynamic Graphs. *Proceedings of the VLDB Endowment* (2018).
- [54] Deevashwer Rathee, Mayank Rathee, Rahul Kranti Kiran Goli, Divya Gupta, Rahul Sharma, Nishanth Chandran, and Aseem Rastogi. 2021. SIRNN: A Math Library for Secure RNN Inference. In *IEEE Symposium on Security and Privacy (S&P)*. IEEE.
- [55] Leyla Roohi, Benjamin IP Rubinstein, and Vanessa Teague. 2019. Differentially-private Two-party Egocentric Betweenness Centrality. In *IEEE INFOCOM Conference on Computer Communications*. IEEE.
- [56] Stephen Tu M Frans Kaashoek Samuel and Madden Nickolai Zeldovich. 2013. Processing Analytical Queries over Encrypted Data. *Proceedings of the VLDB Endowment* (2013).
- [57] Emil Stefanov, Marten van Dijk, Elaine Shi, T-H Hubert Chan, Christopher Fletcher, Ling Ren, Xiangyao Yu, and Srinivas Devadas. 2018. Path ORAM: an extremely simple oblivious RAM protocol. *Journal of the ACM (JACM)* (2018).
- [58] Adithya Vadapalli, Ryan Henry, and Ian Goldberg. 2023. DuORAM: A Bandwidth-Efficient Distributed ORAM for 2-and 3-Party Computation. In *USENIX Security Symposium (USENIX Security)*.
- [59] Nikolaj Volgushev, Malte Schwarzkopf, Ben Getchell, Mayank Varia, Andrei Lapets, and Azer Bestavros. 2019. Conclave: Secure Multi-party Computation on Big Data. In *Proceedings of the EuroSys Conference*.
- [60] Songlei Wang, Yifeng Zheng, and Xiaohua Jia. 2024. GraphGuard: Private Time-Constrained Pattern Detection Over Streaming Graphs in the Cloud. In *33rd USENIX Security Symposium (USENIX Security 24)*. USENIX Association.
- [61] Songlei Wang, Yifeng Zheng, Xiaohua Jia, Qian Wang, and Cong Wang. 2023. MAGO: Maliciously Secure Subgraph Counting on Decentralized Social Graphs. *IEEE Transactions on Information Forensics and Security* (2023).
- [62] Songlei Wang, Yifeng Zheng, Xiaohua Jia, and Xun Yi. 2022. PeGraph: A System for Privacy-Preserving and Efficient Search Over Encrypted Social Graphs. *IEEE Transactions on Information Forensics and Security (TIFS)* (2022). <https://doi.org/10.1109/TIFS.2022.3201392>
- [63] Wai Kit Wong, Ben Kao, David Wai Lok Cheung, Rongbin Li, and Siu Ming Yiu. 2014. SDB:Secure Query Processing with Data Interoperability in A Cloud Database Environment. In *Proceedings of the ACM SIGMOD international conference on Management of data*.
- [64] Lyu Xu, Byron Choi, Yun Peng, Jianliang Xu, and Sourav S Bhowmick. 2023. A framework for privacy preserving localized graph pattern query processing. *Proceedings of the ACM SIGMOD international conference on Management of data* (2023).
- [65] Jaewon Yang and Jure Leskovec. 2012. Defining and Evaluating Network Communities Based on Ground-truth. In *Proceedings of the ACM SIGKDD Workshop on Mining Data Semantics*.
- [66] A. C. Yao. 1986. How to Generate and Exchange Secrets. In *27th Annual Symposium on Foundations of Computer Science (FOCS)*.
- [67] Samee Zahur, Xiao Wang, Mariana Raykova, Adrià Gascón, Jack Doerner, David Evans, and Jonathan Katz. 2016. Revisiting square-root ORAM: efficient random access in multi-party computation. In *IEEE Symposium on Security and Privacy (S&P)*. IEEE.

A Prefix-based ORAM.Access

The original Square-root ORAM [67] uses a $O(n)$ rounds method in the last level of its recursive ORAM (GetPosBase function, in Section D, Figure 6), and in GORAM, we optimize it to $O(\log(n))$ rounds. The interfaces and the methods are shown in Algorithm 5, keeping the same notations as the original Square-root ORAM.

The complicated part in Square-root ORAM is the extraction of the first unused element in the last level ORAM obliviously as the used elements are defined by users access patterns. Algorithm 5 locates this information by constructing $\llbracket \text{fZero} \rrbracket$ (first unused element) leveraging the prefix-computations (Lines 1-6), propagating *whether there exist 1 in $\llbracket \text{notUsed} \rrbracket$ before my location, including my location* to the following elements obliviously. After line 6, $\llbracket \text{fZero} \rrbracket$ contains a successive $\llbracket 0 \rrbracket$ and follows with $\llbracket 1 \rrbracket$, and the last $\llbracket 1 \rrbracket$ indicates the element which is the first unused element, *i.e.*, the first zero in $\llbracket \text{Used} \rrbracket$, the first one in $\llbracket \text{notUsed} \rrbracket$. Then, we obliviously transfers the previous $\llbracket 1 \rrbracket$ to $\llbracket 0 \rrbracket$ by a differential XOR (Lines 7-8). Note that $\llbracket \text{fZero} \rrbracket$ corresponds to the $\llbracket s_2 \rrbracket$ while not considering $\llbracket \text{fake} \rrbracket$ in the original Square-root ORAM.

Algorithm 5: GetPosBase

Inputs : ORAM in the last level containing T blocks, $\llbracket i \rrbracket$ denote the secret index in this level, $\llbracket \text{fake} \rrbracket$.

Output : Physical index p .

// For $\llbracket s_2 \rrbracket$ without $\llbracket \text{fake} \rrbracket$ in [67]

- 1 $\llbracket \text{notUsed} \rrbracket \leftarrow \text{ORAM}.\llbracket \text{Used} \rrbracket$;
- 2 $\llbracket \text{fZero} \rrbracket \leftarrow \llbracket [0, \text{notUsed}_0, \text{notUsed}_1, \dots, \text{notUsed}_{T-2}] \rrbracket$;
- 3 **for** $i \leftarrow 0$ **to** $\lfloor \log_2(T) \rfloor$ **do**
- 4 $s = 2^i$ denoting the stride;
- 5 $\llbracket \text{fZero} \rrbracket_{s:T} \leftarrow \text{OR}(\llbracket \text{fZero} \rrbracket_{s:T}, \llbracket \text{fZero} \rrbracket_{0:T-s})$;
- 6 **end**
- 7 $\llbracket \text{fZero} \rrbracket.\text{append}(\llbracket 1 \rrbracket)$;
- 8 $\llbracket \text{fZero} \rrbracket_{0:T} \leftarrow \text{XOR}(\llbracket \text{fZero} \rrbracket_{0:T}, \llbracket \text{fZero} \rrbracket_{1:T+1})$;
- // Update $\llbracket \text{Used} \rrbracket$*
- // For $\llbracket s_1 \rrbracket$ without $\llbracket \text{fake} \rrbracket$ in [67]*
- 9 $\llbracket s_1 \rrbracket \leftarrow \text{EQ}(\text{expanded}(\llbracket i \rrbracket), [0, 1, \dots, T-1])$;
- // Considering $\llbracket \text{fake} \rrbracket$*
- 10 $\llbracket \text{mask} \rrbracket \leftarrow \llbracket s_1 \rrbracket$ if $\llbracket \text{fake} \rrbracket$ else $\llbracket \text{fZero} \rrbracket$ obliviously;
- // Update $\llbracket \text{Used} \rrbracket$*
- 11 $\text{ORAM}.\llbracket \text{Used} \rrbracket = \text{OR}(\llbracket \text{mask} \rrbracket, \text{ORAM}.\llbracket \text{Used} \rrbracket)$;
- // Get the corresponding index*
- 12 $\llbracket \text{index} \rrbracket \leftarrow \text{DOT}(\text{ORAM}.\llbracket \text{Data} \rrbracket, \llbracket \text{mask} \rrbracket)$;
- 13 Reveal $p \leftarrow$ index in plaintext ;
- 14 **return** p ;

Algorithm 6: UniqueNeighborsCount

Inputs : Target vertex $\llbracket v \rrbracket$ and the target block ID $\llbracket i \rrbracket = \llbracket [r \frac{e}{k}] \rrbracket$.

Output : $\llbracket \text{num} \rrbracket^A$, the number of v 's unique outing neighbors.

// Sub-graph extraction.

- 1 Fetch the target edge blocks $\llbracket B \rrbracket \leftarrow \text{VORAM.access}(\llbracket i \rrbracket)$, where $\llbracket B \rrbracket$ contains (bl) source_nodes and dest_nodes;
- // Parallely sub-graph process.*
- // 1) Mask-out the non-neighbors.*
- 2 Construct $\llbracket \vec{v} \rrbracket$ by expanding $\llbracket v \rrbracket$ bl times;
- 3 Compute $\llbracket \text{mask} \rrbracket \leftarrow \text{EQ}(\llbracket \vec{v} \rrbracket, \llbracket B \rrbracket.\text{source_nodes})$;
- 4 Compute $\llbracket \text{candidate} \rrbracket \leftarrow \text{MUL}(\llbracket \text{mask} \rrbracket, \llbracket B \rrbracket.\text{dest_nodes})$;
- // 2) De-duplicate neighbors.*
- 5 $\llbracket \text{same_mask} \rrbracket \leftarrow \text{EQ}(\llbracket \text{candidate} \rrbracket_{[1:]}, \llbracket \text{candidate} \rrbracket_{[-1:]})$;
- 6 $\llbracket \text{same_mask} \rrbracket.\text{append}(\llbracket 1 \rrbracket)$;
- 7 $\llbracket \text{mask} \rrbracket \leftarrow \text{MUL}(\llbracket \text{same_mask} \rrbracket, \llbracket \text{mask} \rrbracket)$;
- // 3) Aggregating for the final outcomes.*
- 8 Compute $\llbracket \text{mask} \rrbracket^A \leftarrow \text{B2A}(\llbracket \text{mask} \rrbracket)$;
- 9 **while** $\lceil \frac{l}{2} \rceil \geq 1$ **do**
- 10 Pads $\llbracket 0 \rrbracket^A$ to $\llbracket \text{mask} \rrbracket^A$ to be even ;
- 11 Split $\llbracket \text{mask} \rrbracket^A$ half-by-half to $\llbracket \text{mask} \rrbracket_1^A$ and $\llbracket \text{mask} \rrbracket_r^A$;
- 12 Aggregate $\llbracket \text{mask} \rrbracket^A \leftarrow \text{ADD}(\llbracket \text{mask} \rrbracket_1^A, \llbracket \text{mask} \rrbracket_r^A)$;
- 13 $l = \text{len}(\llbracket \text{mask} \rrbracket^A) / 2$;
- 14 **end**
- 15 $\llbracket \text{num} \rrbracket^A = \llbracket \text{mask} \rrbracket^A$;
- 16 **return** $\llbracket \text{num} \rrbracket^A$;

Lines 9 corresponds to $\llbracket s_1 \rrbracket$ of Square-root ORAM, indicating which element corresponding to the cipher index $\llbracket i \rrbracket$. Note that before Line 10, there are only $\llbracket 1 \rrbracket$ in $\llbracket \text{fZero} \rrbracket$ and $\llbracket s_1 \rrbracket$ and the $\llbracket 1 \rrbracket$

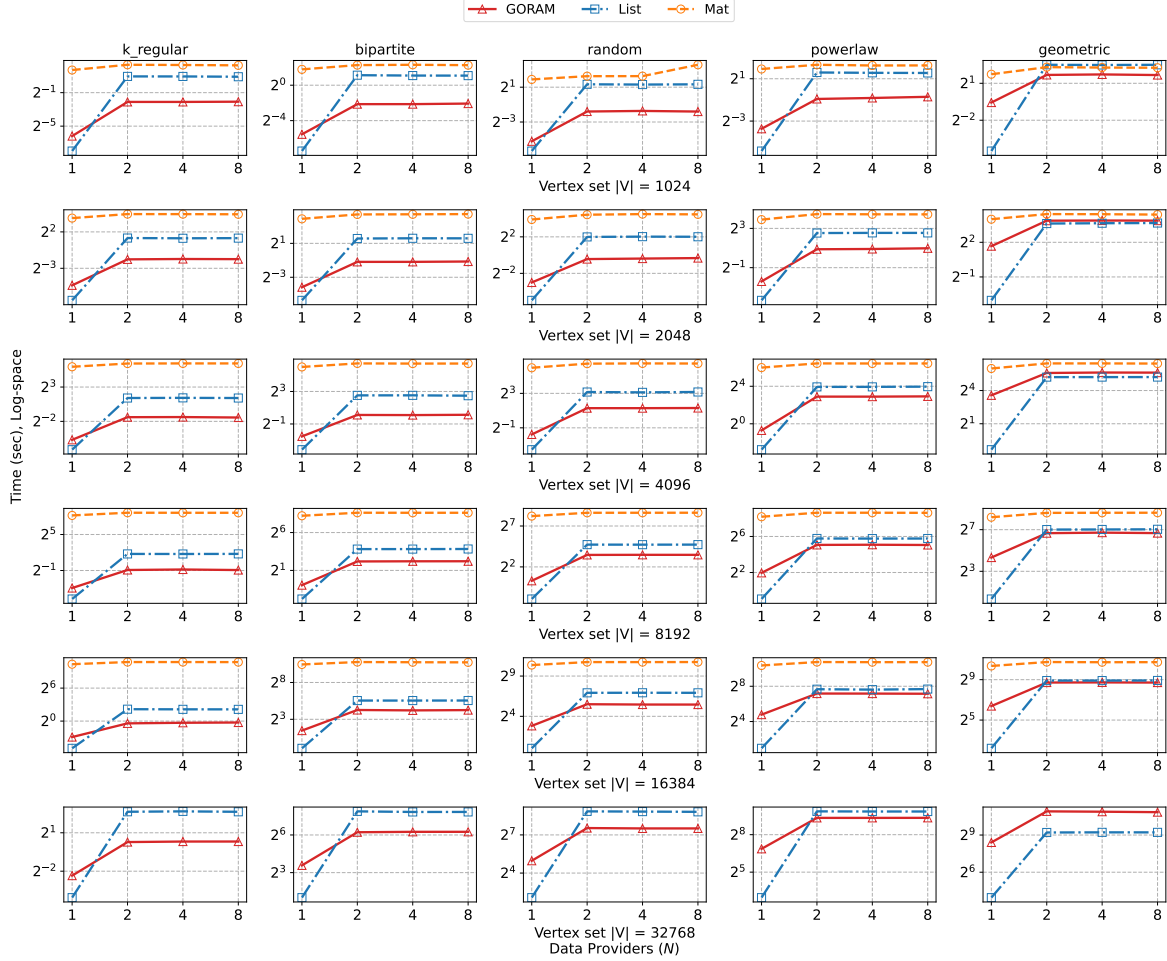


Figure 12: Full Evaluation of Offline Graph Integration (Multiple Data Providers)

indicates the expected element for $\llbracket \text{fake} \rrbracket$ is false or true use cases. We obviously select $\llbracket \text{fZero} \rrbracket$ or $\llbracket s_1 \rrbracket$ based on $\llbracket \text{fake} \rrbracket$ and obtain the $\llbracket \text{mask} \rrbracket$. Note that the $\llbracket 1 \rrbracket$ in $\llbracket \text{mask} \rrbracket$ indicates the to-be-use elements location, therefore we update $\text{ORAM}.\llbracket \text{Used} \rrbracket$ afterwards (Line 11). Then, we get the corresponding element in $\text{ORAM}.\llbracket \text{Data} \rrbracket$ using dot-product, *i.e.*, only the elements corresponding to $\llbracket 1 \rrbracket$ of $\llbracket \text{mask} \rrbracket$ is preserved, which is the expecting physical index.

B Other Queries

UniqueNeighborsCount is shown in Algorithm 6, which adds a de-duplication phase between the sub-graph extraction and aggregation phases, updating the $\llbracket \text{mask} \rrbracket$ eliminating the duplicate neighbors (Lines 2-7). Specifically, the de-duplication procedure is similar to `NeighborsGet` while do not extract the real neighbors.

C Full Offline Construction Evaluation

Figure 6 shows the offline construction cost of multiple data providers with varied graph sizes.